USGS
science for a changing world

Studies by the U.S. Geological Survey in Alaska, 2011

Lithofacies, Age, Depositional Setting, and Geochemistry of the Otuk Formation in the Red Dog District, Northwestern Alaska

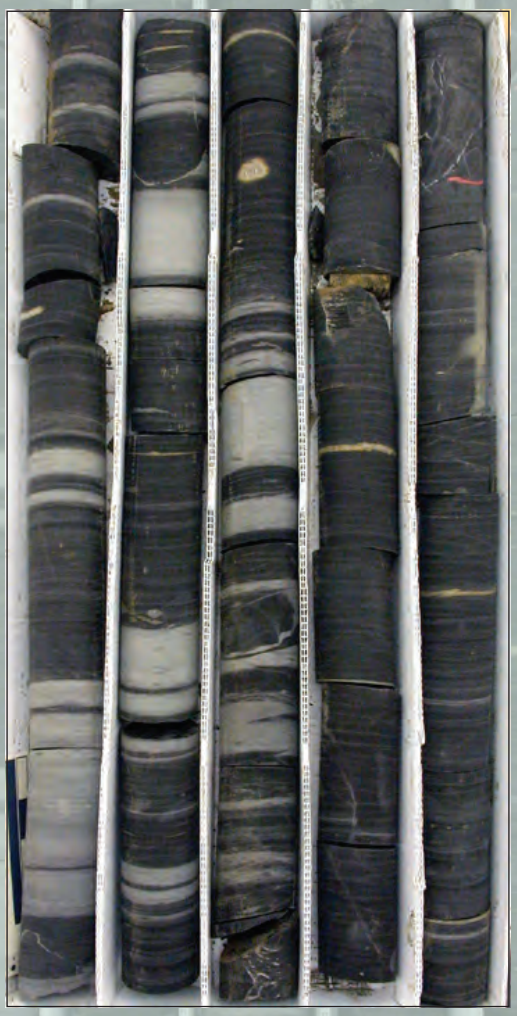

Professional Paper 1795–B

U.S. Department of the Interior
U.S. Geological Survey

Cover image. Photograph of core from the shale member of the Otuk Formation in diamond-drill hole (DDH) 927. The alternating black and light-gray shale seen in this core are very typical of the Otuk in DDH 927.

Studies by the U.S. Geological Survey in Alaska, 2011

Lithofacies, Age, Depositional Setting, and Geochemistry of the Otuk Formation in the Red Dog District, Northwestern Alaska

By Julie A. Dumoulin, Robert C. Burruss, and Charles D. Blome

Professional Paper 1795–B

U.S. Department of the Interior
U.S. Geological Survey

U.S. Department of the Interior
SALLY JEWELL, Secretary

U.S. Geological Survey
Suzette M. Kimball, Acting Director

U.S. Geological Survey, Reston, Virginia: 2013

For more information on the USGS—the Federal source for science about the Earth, its natural and living resources, natural hazards, and the environment, visit http://www.usgs.gov or call 1–888–ASK–USGS.

For an overview of USGS information products, including maps, imagery, and publications, visit http://www.usgs.gov/pubprod

To order this and other USGS information products, visit http://store.usgs.gov

Suggested citation:
Dumoulin, J.A., Burruss, R.C., and Blome, C.D., 2013, Lithofacies, age, depositional setting, and geochemistry of the Otuk Formation in the Red Dog District, northwestern Alaska: U.S. Geological Survey Professional Paper 1795–B, 32 p.

Contents

Figures

Tables

Studies by the U.S. Geological Survey in Alaska, 2011
Edited by Julie A. Dumoulin and Cynthia Dusel-Bacon
U.S. Geological Survey Professional Paper 1795–B

Lithofacies, Age, Depositional Setting, and Geochemistry of the Otuk Formation in the Red Dog District, Northwestern Alaska

By Julie A. Dumoulin, Robert C. Burruss, and Charles D. Blome

Abstract

Complete penetration of the Otuk Formation in a continuous drill core (diamond-drill hole, DDH 927) from the Red Dog District illuminates the facies, age, depositional environment, source rock potential, and isotope stratigraphy of this unit in northwestern Alaska. The section, in the Wolverine Creek plate of the Endicott Mountains Allochthon (EMA), is ~82 meters (m) thick and appears structurally uncomplicated. Bedding dips are generally low and thicknesses recorded are close to true thicknesses. Preliminary synthesis of sedimentologic, paleontologic, and isotopic data suggests that the Otuk succession in DDH 927 is a largely complete, albeit condensed, marine Triassic section in conformable contact with marine Permian and Jurassic strata.

The Otuk Formation in DDH 927 gradationally overlies gray siliceous mudstone of the Siksikpuk Formation (Permian, based on regional correlations) and underlies black organic-rich mudstone of the Kingak(?) Shale (Jurassic?, based on regional correlations). The informal shale, chert, and limestone members of the Otuk are recognized in DDH 927, but the Jurassic Blankenship Member is absent. The lower (shale) member consists of 28 m of black to light gray, silty shale with as much as 6.9 weight percent total organic carbon (TOC). Thin limy layers near the base of this member contain bivalve fragments (*Claraia* sp.?) consistent with an Early Triassic (Griesbachian-early Smithian) age. Gray radiolarian chert dominates the middle member (25 m thick) and yields radiolarians of Middle Triassic (Anisian and Ladinian) and Late Triassic (Carnian-late middle Norian) ages. Black to light gray silty shale, like that in the lower member, forms interbeds that range from a few millimeters to 7 centimeters in thickness through much of the middle member. A distinctive, 2.4-m-thick interval of black shale and calcareous radiolarite ~17 m above the base of the member has as much as 9.8 weight percent TOC, and a 1.9-m-thick interval of limy to cherty mudstone immediately above this contains radiolarians, foraminifers, conodonts, and halobiid bivalve fragments. The upper (limestone) member (29 m thick) is lime mudstone with monotid bivalves and late Norian radiolarians, overlain by gray chert that contains Rhaetian (latest Triassic) radiolarians; Rhaetian strata have not previously been documented in the Otuk. Rare gray to black shale interbeds in the upper member have as much as 3.4 weight percent TOC. At least 35 m of black mudstone overlies the limestone member; these strata lack interbeds of oil shale and chert that are characteristic of the Blankenship, and instead they resemble the Kingak Shale. Vitrinite reflectance values (2.45 and 2.47 percent R_o) from two samples of black shale in the chert member indicate that these rocks reached a high level of thermal maturity within the dry gas window.

Regional correlations indicate that lithofacies in the Otuk Formation vary with both structural and geographic position. For example, the shale member of the Otuk in the Wolverine Creek plate includes more limy layers and less barite (as blades, nodules, and lenses) than equivalent strata in the structurally higher Red Dog plate of the EMA, but it has fewer limy layers than the shale member in the EMA ~450 kilometers (km) to the east at Tiglukpuk Creek. The limestone member of the Otuk is thicker in the Wolverine Creek plate than in the Red Dog plate and differs from this member in EMA sections to the east in containing an upper cherty interval that lacks monotids; a similar interval is seen at the top of the Otuk Formation ~125 km to the west (Lisburne Peninsula). Our observations are consistent with the interpretations of previous researchers that Otuk facies become more distal in higher structural positions and that within a given structural level more distal facies occur to the west. Recent paleogeographic reconstructions indicate that the Otuk accumulated at a relatively high paleolatitude with a bivalve fauna typical of the Boreal realm.

A suite of $\delta^{13}C_{org}$ (carbon isotopic composition of carbon) data (n=38) from the upper Siksikpuk Formation through the Otuk Formation and into the Kingak(?) Shale in DDH 927 shows a pattern of positive and negative excursions similar to those reported elsewhere in Triassic strata. In particular, a distinct negative excursion at the base of the Otuk (from −23.8 to −31.3‰ (permil, or parts per thousand)) likely correlates with a pronounced excursion that marks the Permian-Triassic boundary at many localities worldwide. Another feature of the Otuk $\delta^{13}C_{org}$ record that may correlate globally is a series of negative and positive excursions in the lower member. At the top of the Otuk in DDH 927, the $\delta^{13}C_{org}$ values are extremely low and may correlate with a negative excursion that is widely observed at the Triassic-Jurassic boundary.

Introduction

The Otuk Formation (Triassic-Jurassic) is a potential hydrocarbon source rock (Lillis and others, 2002; Lillis, 2003) that is widely distributed in outcrop and subsurface across northern Alaska (fig. 1). This paper documents the lithofacies, age, and depositional setting of the Otuk in the Red Dog District, northwestern Alaska (figs. 1, 2) and compares its facies and stratigraphy with those of correlative sections to the west (Cape Lisburne) and east (central Brooks Range). Also discussed are some aspects of the organic and isotope geochemistry of the Otuk.

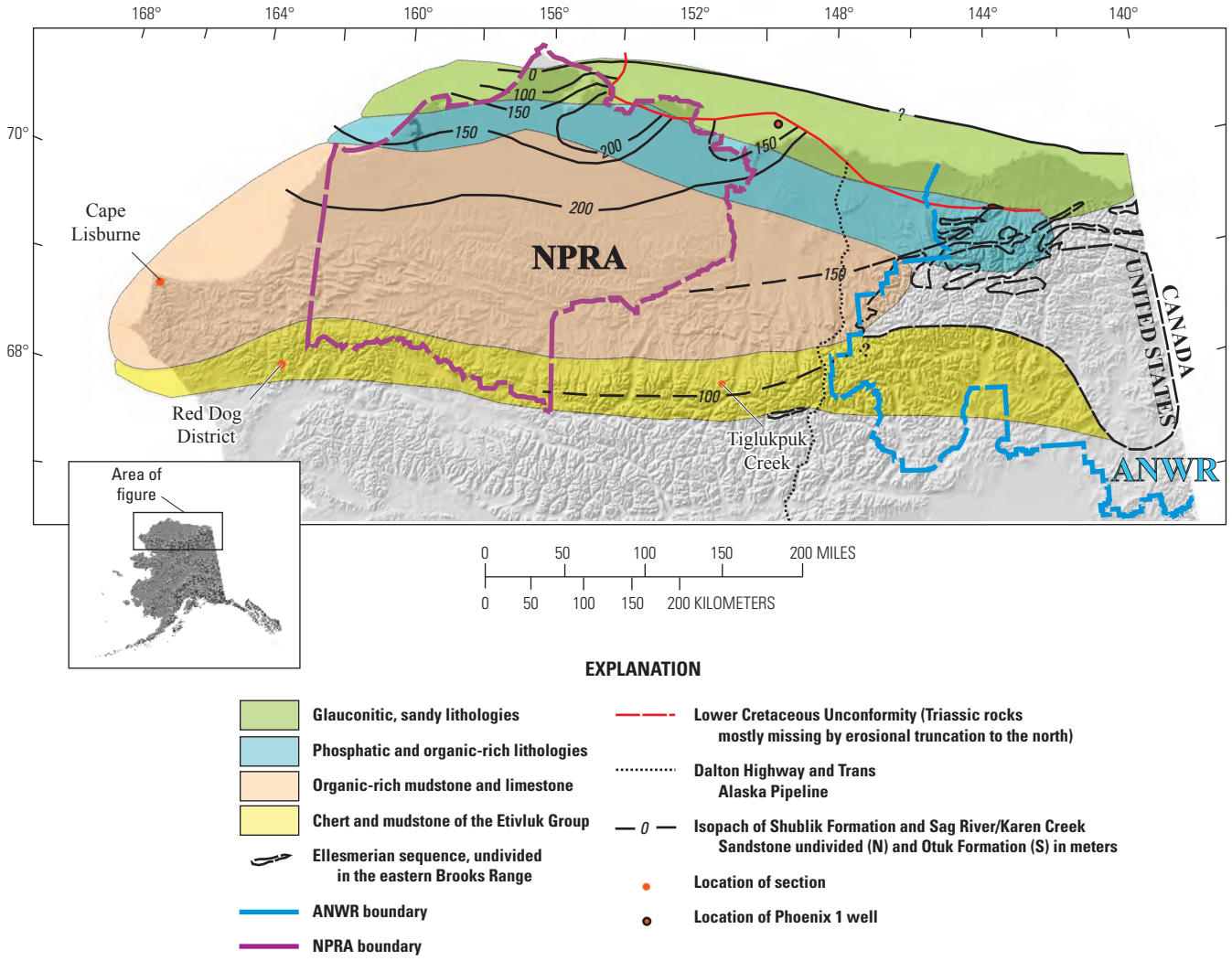

Figure 1. Map showing distribution of generalized lithofacies and isopachs of selected Triassic rocks across northern Alaska, outcrop and subsurface sections discussed in the text, and boundaries of the National Petroleum Reserve in Alaska (NPRA), and the Arctic National Wildlife Refuge (ANWR). Otuk Formation (beige and yellow facies) occurs in outcrop from Cape Lisburne to the southeastern Brooks Range; Shublik Formation (green, blue, and beige facies) occurs in outcrop mainly in the northeastern Brooks Range but is widely distributed in the subsurface. The transition between the two units has not been precisely located. Modified from Kelly and others (2007). Note that the placement of the zero isopach offshore is uncertain.

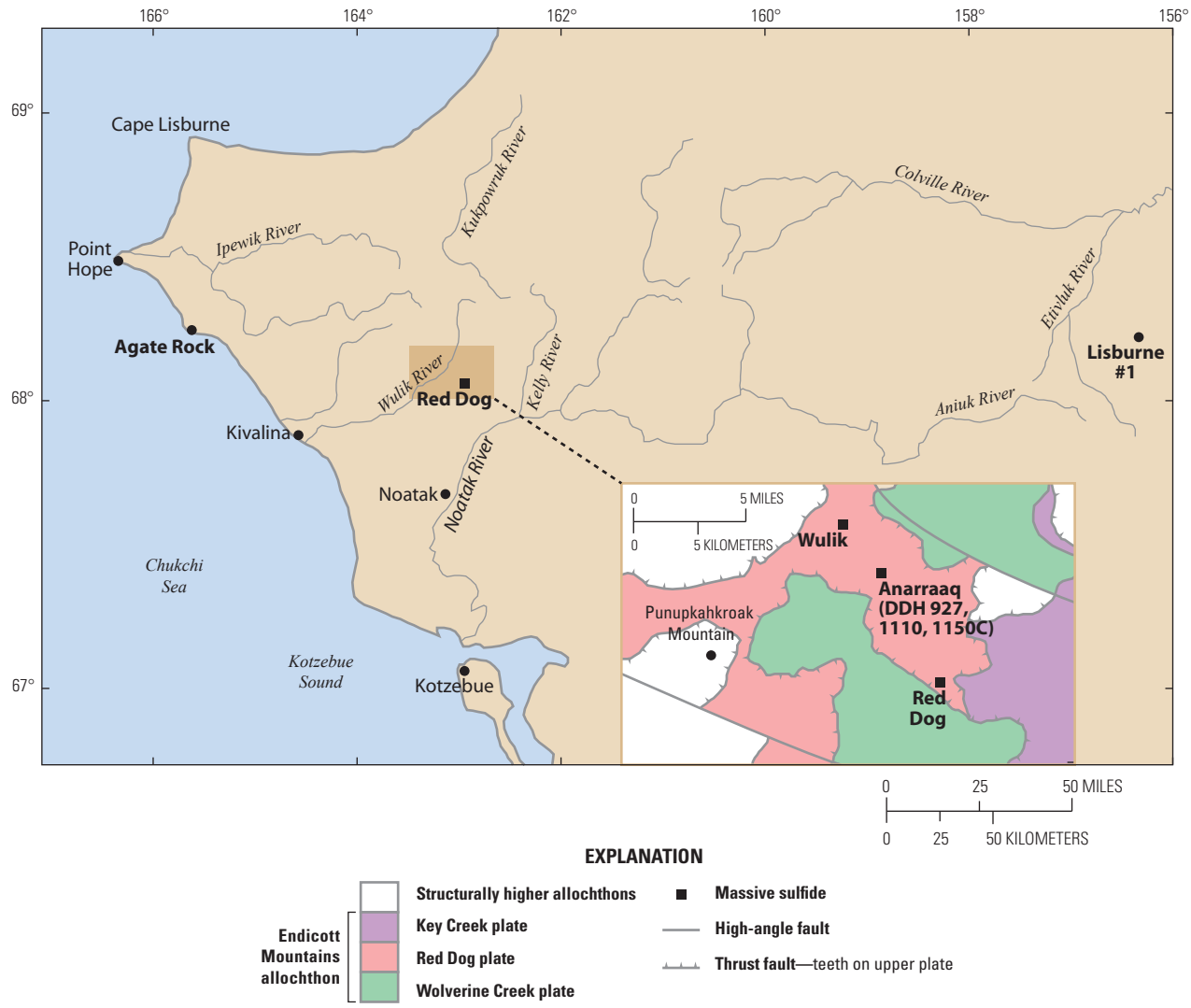

Figure 2. Map of northwestern Alaska showing location of study area (brown rectangle); inset shows plates of the Endicott Mountains Allochthon (EMA) in area of the Red Dog Mine (De Vera and others, 2004). DDH, diamond-drill hole. Otuk Formation was cored in DDHs 927, 1110, and 1150C.

Carboniferous facies in northern Alaska have long been known to vary with shifts in geographic and structural settings (Mayfield and others, 1988; Dumoulin and others, 2004). Herein we provide the first detailed description of the Otuk Formation in the western Brook Range, and demonstrate that its facies also show differences linked to geographic position and structural level. In addition, we document significant positive and negative excursions in $\delta^{13}C_{org}$ within the Otuk that are similar to those reported in other Triassic sections worldwide. The cause of these excursions remains a subject of intense debate (Tanner, 2010). Our preliminary synthesis of sedimentologic, paleontologic, and isotopic data suggests that the Otuk succession in diamond-drill hole (DDH) 927 is a largely complete marine Triassic section in conformable contact with marine Permian and Jurassic strata.

Structural, Stratigraphic, and Paleogeographic Setting

Our study focuses on a subsurface section of the Otuk Formation in the vicinity of the Red Dog Mine in northwestern Alaska (figs. 1, 2). Paleozoic and Mesozoic strata in this area, and throughout much of the western and central Brooks Range, are exposed in a series of discrete structural allochthons that formed during the late Mesozoic and Tertiary Brooks Range orogeny. Individual allochthons are imbricated internally and are made up of plates and thrust sheets, some of which are named. We use the terminology of Young (2004) for these structural features.

Triassic and Jurassic facies vary widely across northern Alaska (fig. 1) and a complex stratigraphic nomenclature has developed to encompass this variation (fig. 3). These rocks are part of the upper Ellesmerian megasequence of Hubbard and others (1987). In outcrops of the northeastern Brooks Range, and in much of the subsurface beneath the North Slope of Alaska, Triassic rocks are considered to be parautochthonous (Young, 2004) and consist of siliciclastic deposits (Ivishak Formation of the Sadlerochit Group) overlain by a relatively thin, silty sandstone (called Karen Creek Sandstone in outcrop and Sag River Sandstone in subsurface) and calcareous siltstone and sandstone, limestone, and mudstone of the Shublik Formation (Detterman and others, 1975; Parrish and others, 2001). These Triassic strata overlie Permian siliciclastic rocks of the Echooka Formation and underlie dark shale and lesser siltstone of the Jurassic through Lower Cretaceous Kingak Shale (Detterman and others, 1975).

Lower Mesozoic strata of the Endicott Mountains Allochthon (EMA) occur throughout the central and western Brooks Range and represent generally finer grained, more distal facies equivalents of coeval units to the north and east (figs. 1, 3). The Otuk Formation of the Etivluk Group (Mull and others, 1982) consists mainly of shale, chert, and lime mudstone and overlies similar facies of the Pennsylvanian-Permian Siksikpuk Formation. In much of the EMA, the uppermost part of the Otuk is of Early and Middle Jurassic age and consists of organic-rich shale of the Blankenship Member. The Blankenship is largely absent, however, from sections that represent the lowest structural level of the EMA, called the Wolverine Creek plate in the west (Red Dog area) and the Ivotuk plate farther east (west-central Brooks Range). In these sections, Triassic rocks of the Otuk are overlain by undated dark mudstone that resembles the Kingak Shale (Young, 2004; Dumoulin and White, 2005).

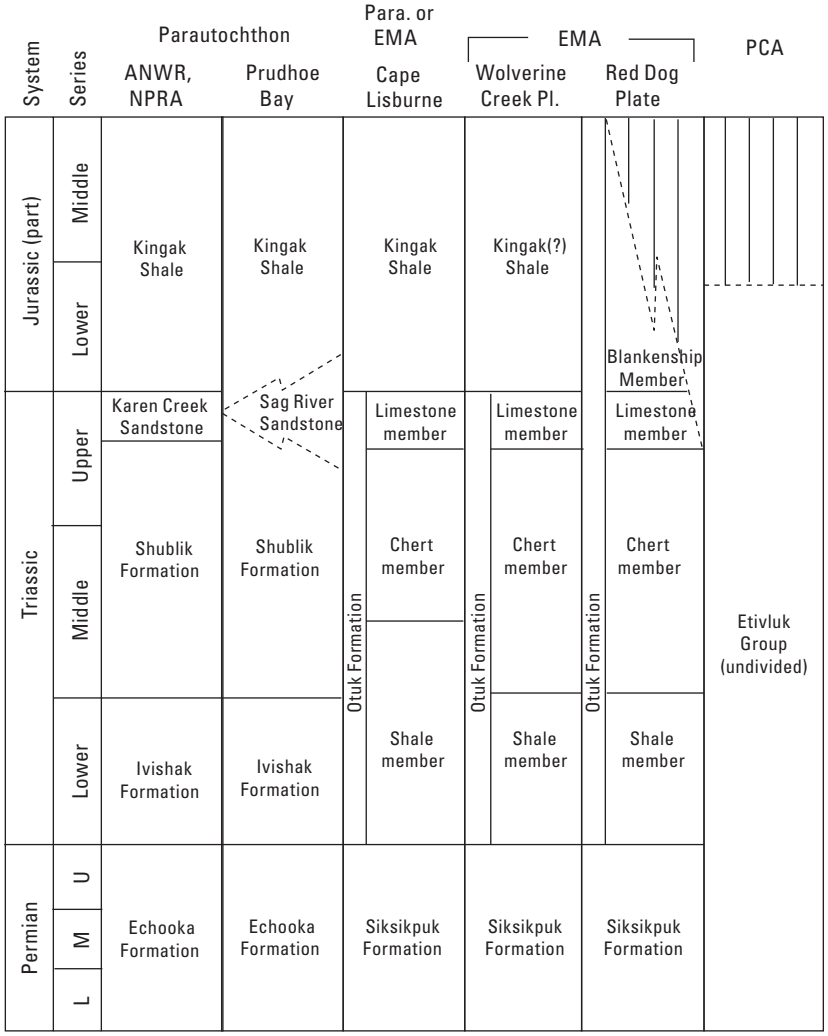

Figure 3. Diagram showing stratigraphic nomenclature for Permian-Jurassic strata in selected areas of northern Alaska; Karen Creek Sandstone recognized in ANWR (Arctic National Wildlife Refuge) but not in NPRA (National Petroleum Reserve in Alaska). From information in Blome and others (1988), Parrish and others (2001), Moore and others (2002), Young (2004), and Dumoulin and White (2005). L, Lower; M, Middle; U, Upper; Para., Parautochthon; Pl., Plate; EMA, Endicott Mountains Allochthon; PCA, Picnic Creek Allochthon.

Lower Mesozoic strata in the Cape Lisburne area of northwestern Alaska (fig. 2) were considered parautochthonous by Young (2004) but were included in the EMA by Mayfield and others (1988). These rocks (Moore and others, 2002) are similar to coeval strata in the Wolverine Creek plate (fig. 2) and are described with a virtually identical stratigraphic nomenclature (fig. 3).

Structurally higher allochthons contain lower Mesozoic facies that appear even more distal than those of the EMA. For example, Permian through Lower Jurassic strata in the Picnic Creek Allochthon (PCA; fig. 3) are highly siliceous and generally called Etivluk Group undivided in the western Brooks Range (Blome and others, 1988; Young, 2004).

Triassic rocks of northern Alaska are part of the Arctic Alaska Microplate of Hubbard and others (1987). The paleogeographic history of this microplate remains controversial, but most recent models have shown it as adjacent or attached to North America during the early Mesozoic at a paleolatitude of ~+45–60° (Scotese, 2001; Lawver and others, 2002; Kelly and others, 2007; Colpron and Nelson, 2009). Triassic bivalves from the Otuk Formation and correlative units are part of the Boreal province (for example, McRoberts, 2010) which extends from Siberia through northern Alaska, Arctic Canada, Greenland, and Svalbard.

Lithofacies

In this paper we describe a complete section of the Otuk Formation that was continuously cored in Teck Mining Company's DDH 927, 2.7 kilometers (km) west of the the Anarraaq deposit in the Red Dog District (fig. 2); we also studied the overlying Kingak(?) Shale and the underlying Siksikpuk Formation (upper part) in this drill hole. In addition, we sampled the Kingak(?) and upper Otuk in nearby DDH 1110, which is 1.5 km west of Anarraaq (fig. 2). The drill holes are nearly vertical. Both studied sections are in the Wolverine Creek plate of the EMA, which in this area structurally underlies several thrust-faulted partial repeats of Carboniferous and younger strata in the Red Dog plate of the EMA. A mélange zone marks the contact between the two plates in both drill holes. DDH 927 contains the only complete section of the Otuk that has been cored in the Red Dog District, and thus it provides a unique opportunity to examine Triassic stratigraphy and lithofacies in the western Brooks Range.

Siksikpuk Formation

The Siksikpuk Formation in the EMA of the western Brooks Range is ~70 to 165 meters (m) thick and encompasses four informal subunits—lower, middle, upper, and transitional (Young, 2004). DDH 927 penetrated only the upper two of these subunits. About 27 m (88 feet, ft) of Siksikpuk was drilled in DDH 927.[1] In the Red Dog District, the thickest and most proximal section of the Siksikpuk occurs in the Wolverine Creek plate (Young, 2004).

Upper Subunit

The upper subunit of the Siksikpuk Formation is 9 to 46 m thick and typically consists of greenish-gray and maroon chert, although more proximal (less siliceous) facies occur in the Wolverine Creek plate (Young, 2004). In DDH 927, ~24 m (80 ft) of slightly greenish, medium-gray, locally siliceous mudstone make up the upper subunit (fig. 5). Total organic carbon (TOC) values are uniformly low (0.2 to 0.6 weight percent; fig. 4, table A1). Features observed in thin sections include consistent but minor amounts of disseminated quartz silt to very fine sand, rare agglutinated foraminifers (fig. 5*A*, *B*), and, in some samples, <5 percent disseminated, silt-sized dolomite rhombs. Irregular blebs, veins, and centimeter-thick layers of barite occur throughout the subunit (fig. 5*C*). Pyrite masses, some with barite cores and as much as 2 centimeters (cm) in diameter, are notable in the uppermost meter of section.

Transitional Subunit

A transitional subunit, ≤8 m thick, occurs at the top of the Siksikpuk Formation and is made up mostly of gray and lesser brown or maroon shale and subordinate chert (Young, 2004). In DDH 927, this subunit is ~2.4 m (8 ft) thick and consists of 0.5- to 1-m-thick alternations of medium gray mudstone like that in the upper subunit and organic-rich, dark-gray to black shale typical of the overlying shale member of the Otuk Formation (fig. 5*D*). We selected the base of the transitional subunit at the base of the lowest interbed of dark shale, and the top of the subunit at the top of the highest medium-gray mudstone. The black shale contains locally abundant thin (≤200 micrometers, μm) lenses of silt, as well as several graded layers (as much as 2.5 cm thick) of silt to very fine sand; clasts include chert, quartz, feldspar, and dolomite, as well as possible mudstone and volcanic rock fragments. Pyrite, in local lenses and disseminated grains, and rare muddy laminae rich in radiolarians also occur in the dark shale intervals.

Otuk Formation

The Otuk Formation in the Wolverine Creek plate consists of three subunits that have been informally recognized in the Otuk throughout the Brooks Range (Mull and others, 1982; Bodnar, 1984; Blome and others, 1988; Young, 2004).

[1]Unit thicknesses in drill cores given here have not been corrected for dip and are thus somewhat greater than true thicknesses. Bedding dips recorded on drill logs in the cores sampled are generally less than 40° and through much of the Otuk are 0 to 20°; measured thicknesses are therefore at most 6 to 23 percent greater than true thicknesses. Drill cores are calibrated and archived by Teck Mining Company using English units.

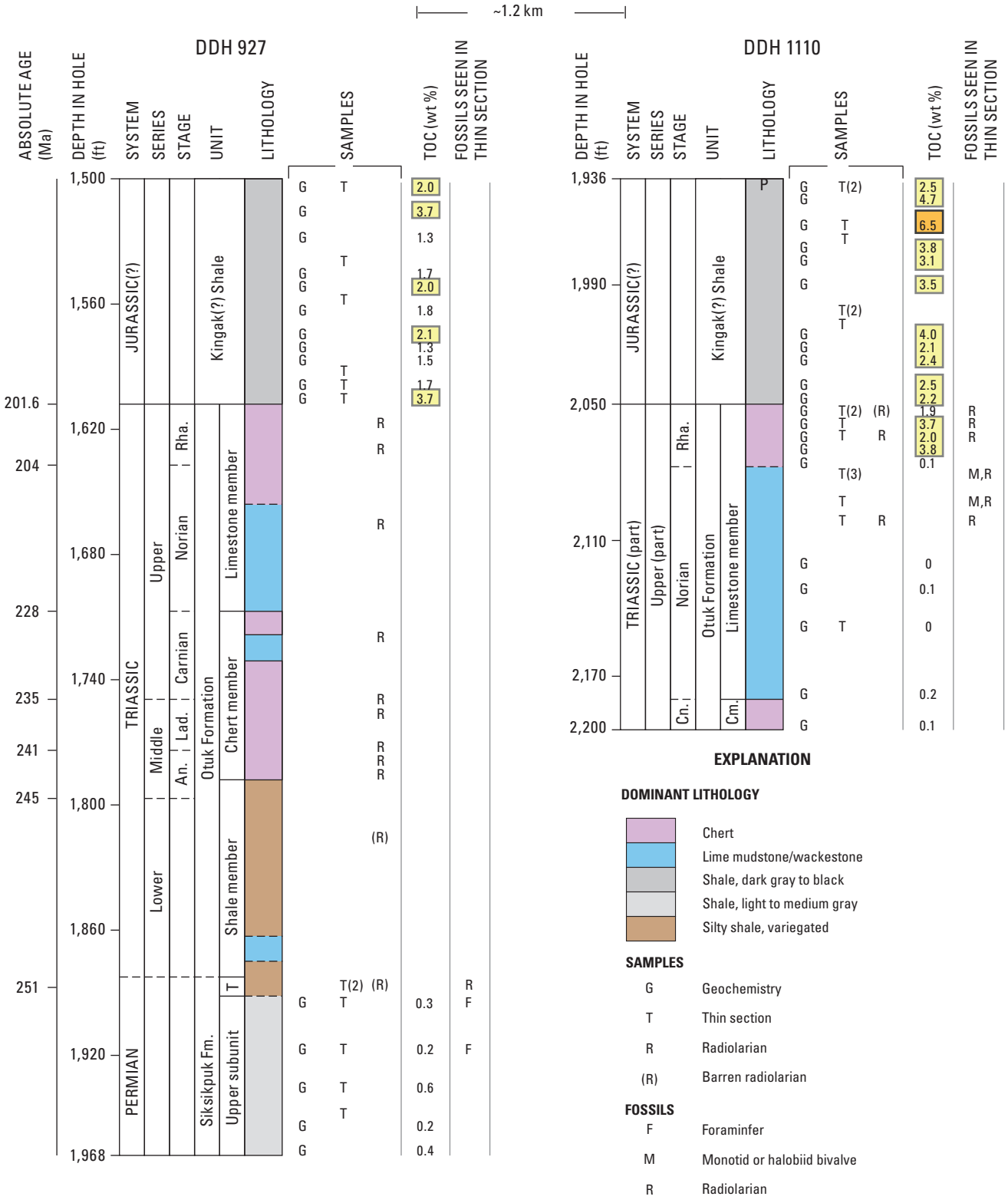

Figure 4. Diagram showing the stratigraphy of the Wolverine Creek plate cored in diamond-drill holes (DDH) 927 (68°09′20″N, 163°01′40″W) and 1110 (68°09′40″N, 163°00′20″W). In both drill holes, the upper surface of the Kingak(?) Shale shown here is a fault, and the base of both sections is the bottom of the hole. See figure 6 for more detailed stratigraphy and sample, fossil, and total organic carbon (TOC) data from the Otuk Formation in DDH 927. TOC values of 2 to 5 weight percent (wt %) are highlighted in yellow; values >5 weight percent are highlighted in orange. Absolute ages from Walker and Geissman (2009). P, paleosol. R in samples column indicates rocks were processed in an attempt to extract radiolarians; R in fossils column indicates radiolarians were observed in thin section. T (in unit column), transitional unit of Siksikpuk Formation; Cm, chert member of Otuk Formation. An., Anisian; Cn, Carnian; Lad., Ladinian, Rha., Rhaetian. Ma, mega-annum; ft, feet.

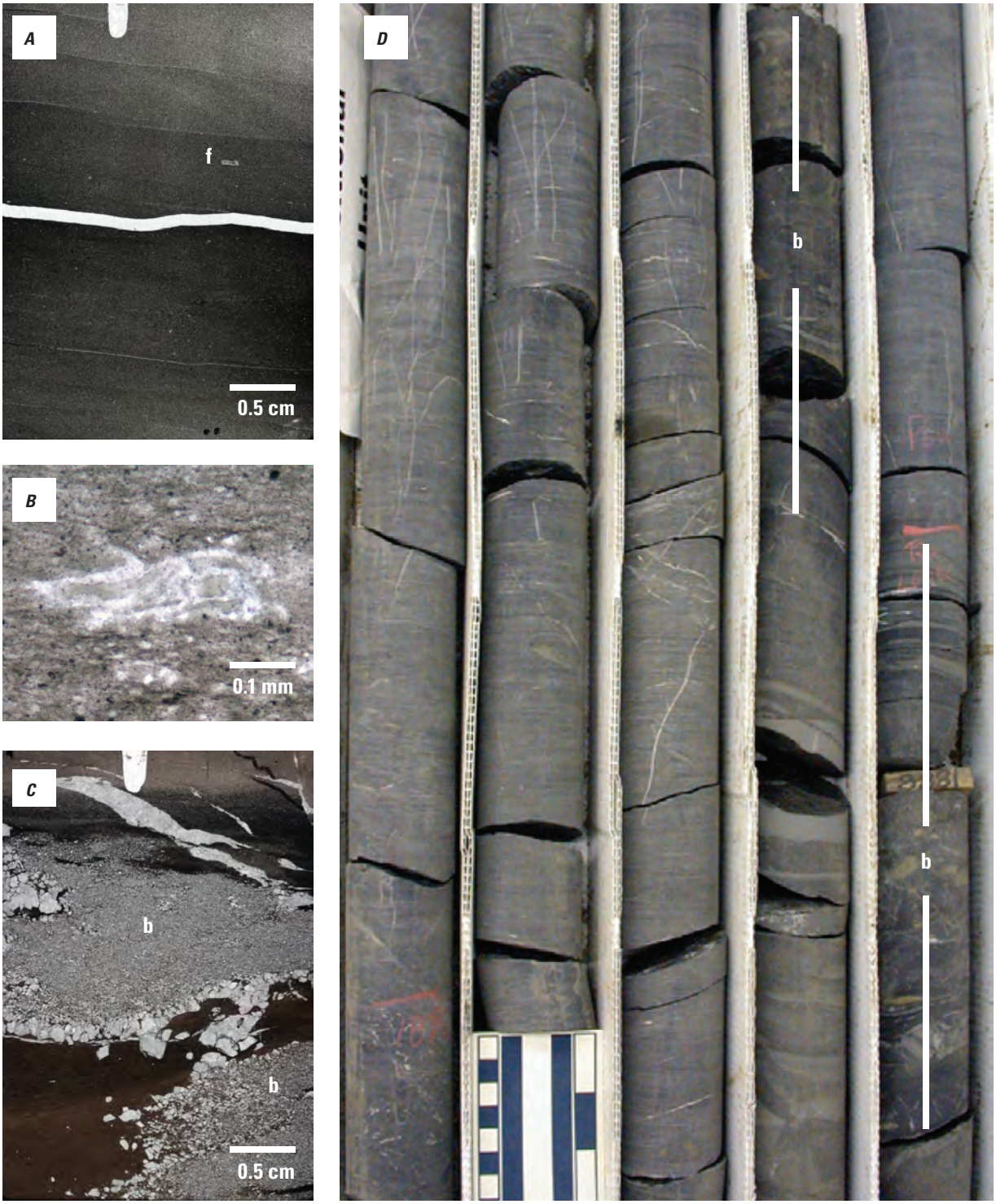

Figure 5. Photographs showing lithologic features of Siksikpuk Formation in diamond-drill hole (DDH) 927. *A*, *C*, thin section scans; *B*, photomicrograph; *D*, core photograph. *A*–*C*, Upper subunit: *A*, Typical gray mudstone with low total organic carbon (TOC) (0.6 weight percent) and rare agglutinated foraminifers (f); 1,917 feet (ft). *B*, Partly flattened agglutinated foraminifer test; 1,917 ft. *C*. Blebs, lenses, and layers of barite (b) are common in this subunit; 1,938 ft. *D*, Transitional subunit consists of gray mudstone typical of the Siksikpuk interbedded with black shale (b) typical of the overlying Otuk Formation; core from 1,880 to 1,889.5 ft (top to left); scale bar units in centimeters (cm) (left) and inches (right). mm, millimeter.

These are, in ascending order, the shale, chert, and limestone members. The formally named uppermost part of the Otuk, the Blankenship Member (Mull and others, 1982), does not occur in either the DDH 927 or DDH 1110 section. Thickness of the Otuk ranges from ~45 to 125 m (Mull and others, 1982; Bodnar, 1984; Young, 2004); the Otuk in DDH 927 is ~82 m (269 ft) thick.

Shale Member

In DDH 927, the shale member is ~28 m (91 ft) thick and consists largely of varicolored silty shale (fig. 6). The shale ranges from light gray to black; intervals of contrasting color ranging from <1 mm to >0.5 m in thickness are a characteristic feature of this member (fig. 7*A*, *D*, *E*). Silt and lesser very fine sand occur throughout the member, both as disseminated grains and concentrated into thin lenses and layers (fig. 7*E–G*). Some silty lenses may be flattened clasts or burrows. Centimeter-thick siltstone layers display parallel laminae, low-angle cross-laminae, and normal size grading (fig. 7*E*). Irregular blebby textures suggestive of partial bioturbation and less common soft sediment deformation features are seen in shale and siltstone. Much of the silt and sand is monocrystalline quartz and white mica (fig. 7*F*). Dolomite rhombs are abundant in some samples (fig. 7*G)*. Plagioclase feldspar and lithic clasts (including chert) were recognized locally, especially in zones with sand-sized detritus.

The main compositional difference between dark and light shale intervals is the abundance of organic matter (figs. 6, 7*D*, table A1). Weight percent TOC in 10 samples of dark-gray to black shale averages 3.6 (range 1.3–6.9), but in 4 samples of light- to medium-gray shale weight percent TOC averages 0.19 (range 0.12–0.25). Barite occurs locally in dark shale near the top of the member, mainly as bladed crystals in layers ≤1 mm thick (fig. 7*H*).

Several calcareous intervals, ~1.2 to 1.8 m thick, occur in the lower half of the member (figs. 6, 7*A*). They consist of abundant calcareous shell debris (fig. 7*B*, *C*) in a matrix of dark, silty mudstone. The shells are mainly prismatic bivalve fragments (*Claraia* sp.?) and are further discussed below. Small brown nodules (phosphatic? chert) occur locally.

Radiolarians are most abundant in the upper third of the member (figs. 6, 7*H*). Most have a matrix of dark mud and are filled with chalcedony. In one sample, radiolarians fill a 1-cm-diameter cylindrical form that may be a burrow. Phosphatic bioclasts (conodonts or ichthyoliths) and possible agglutinated foraminifers were noted in several samples.

Chert Member

The chert member in DDH 927 is ~25 m (83 ft) thick and extends from the base of the lowest chert layer to the base of a lime mudstone interval that is >10 m thick. Medium gray chert is the dominant lithology. Interlayers of silty shale a few millimeters to 7 cm thick occur throughout the member but are particularly abundant in the lower half (fig. 8*A–C*). These shales are identical to those in the shale member and range from black and organic-rich (5.8 weight percent TOC) to light gray and organic-poor (0.2-0.3 weight percent TOC; figs. 6, 8*A*, table A1). Some silty layers appear partly bioturbated (fig. 8*C*). Chert contains rare to abundant radiolarians (ranging from a few to >60 percent) and lesser sponge spicules. Radiolarian tests are generally filled with chalcedony but some contain barite or pyrite. Some layers of radiolarian chert grade upward into shale or siliceous mudstone (fig. 8*B*). Rare phosphatic bioclasts (including probable conodonts) occur locally in both shale and chert. Layers of barite crystals (some with cores made of quartz and pyrite) in a dark mudstone matrix occur at several horizons in the lower half of the member.

There are two distinctive intervals in the upper half of the chert member. The lower of these (dm, figs. 6, 8*D*, *E*) is ~2.4 m of mainly dark gray to black, sooty, calcareous to siliceous mudstone and shale that correlates with the "distinctive marker horizon" described by Young (2004, p. 1291)—a regional marker in the chert member that Young recognized in the EMA and in higher allochthons. Limy layers in this interval contain calcite-replaced radiolarians (fig. 8*E*) and halobiid flat clam fragments in a matrix of fine-grained carbonate. Shales have as much as 9.8 weight percent TOC (fig. 6), the highest value determined in the Otuk Formation in this study. Silt to very fine sand grains occur locally, both disseminated and in lenses and laminae, and include quartz, white mica, dolomite, plagioclase, and sedimentary and volcanic lithic clasts.

Just above this marker horizon, 1.9 m of light-gray to olive-gray, calcareous to dolomitic mudstone, chert, and shale form a second distinctive upper horizon (uh, figs. 6, 8*F–H*). Radiolarians (locally replaced by carbonate or pyrite), calcareous foraminifers, halobiid bivalve fragments, phosphatic bioclasts (including conodonts; table 1, sample 927-1720) and possible calcispheres are sparse but consistently present throughout this interval (fig. 8*F–H*). Fine-grained dolomite rhombs are abundant throughout this zone.

The uppermost part of the chert member in DDH 927 is medium gray chert much like that elsewhere in the member but cut by numerous veins of sparry calcite. Five meters of similar gray chert at the base of DDH 1110 (fig. 4) likely correlates with this interval.

Limestone Member

The limestone member of the Otuk Formation was penetrated in DDHs 927 and 1110 and consists of a limy lower part and a cherty upper part in both drill holes (figs. 4, 6, 9). Locally steep dips observed in core suggest that the member has been structurally thickened, particularly in DDH 1110, where it extends for ~48 m (157 ft). A thickness of ~29 m (95 ft) was logged for the member in DDH 927, which is

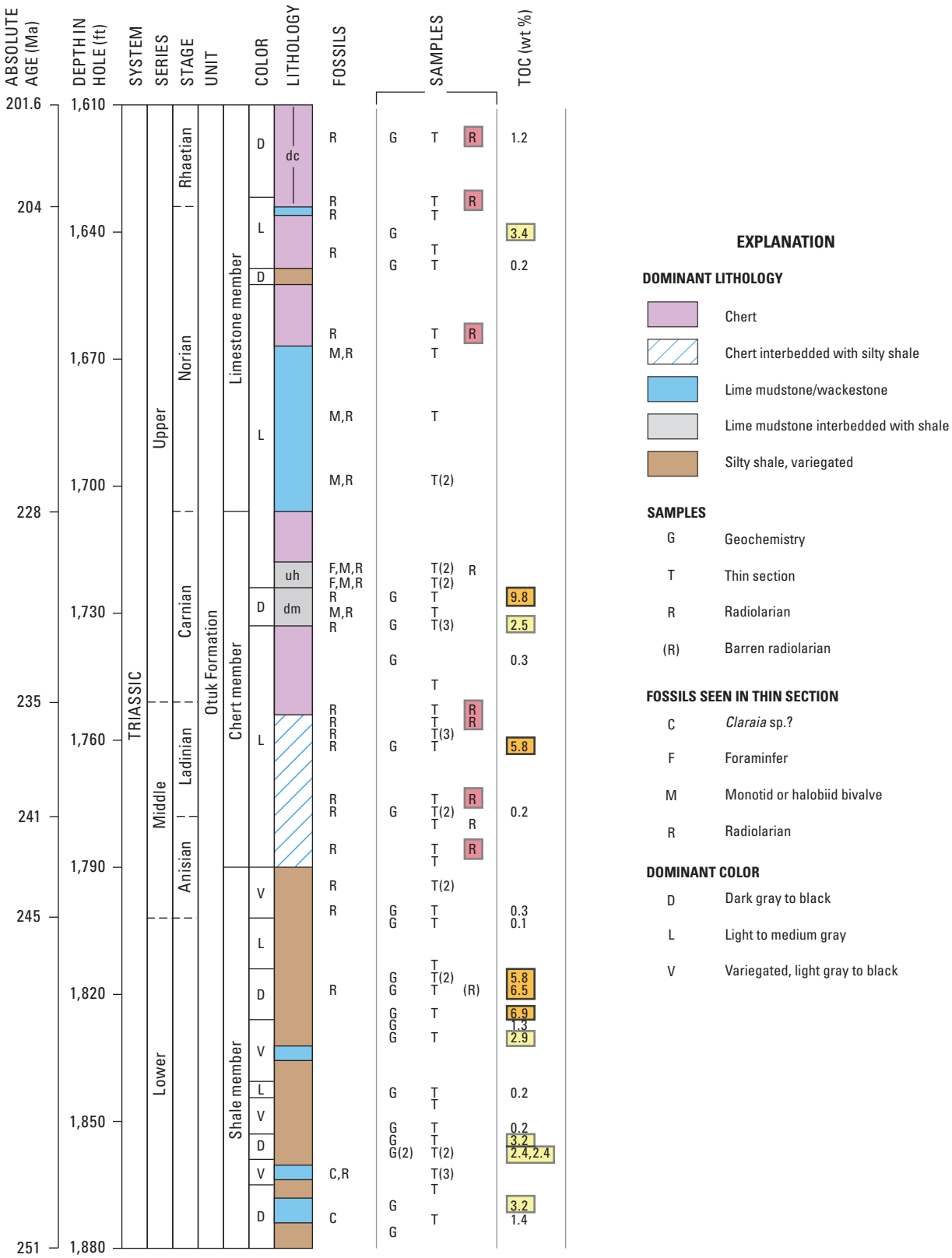

Figure 6. Diagram showing detailed stratigraphy of the Otuk Formation cored in diamond-drill hole (DDH) 927. Radiolarian samples that yielded tightly diagnostic ages (most constrained to zone; see table 1) are highlighted in red; total organic carbon (TOC) values of 2 to 5 weight percent (wt %) are highlighted in yellow; values >5 weight percent are highlighted in orange. dc, dark chert interval; dm, dark marker horizon; uh, upper horizon. Dashed lines indicate that exact placements of stage and series boundaries are uncertain. Probable *Claraia* sp. fragments suggest an age of Griesbachian-early Smithian (see text for discussion). Ma, mega-annum; ft, feet.

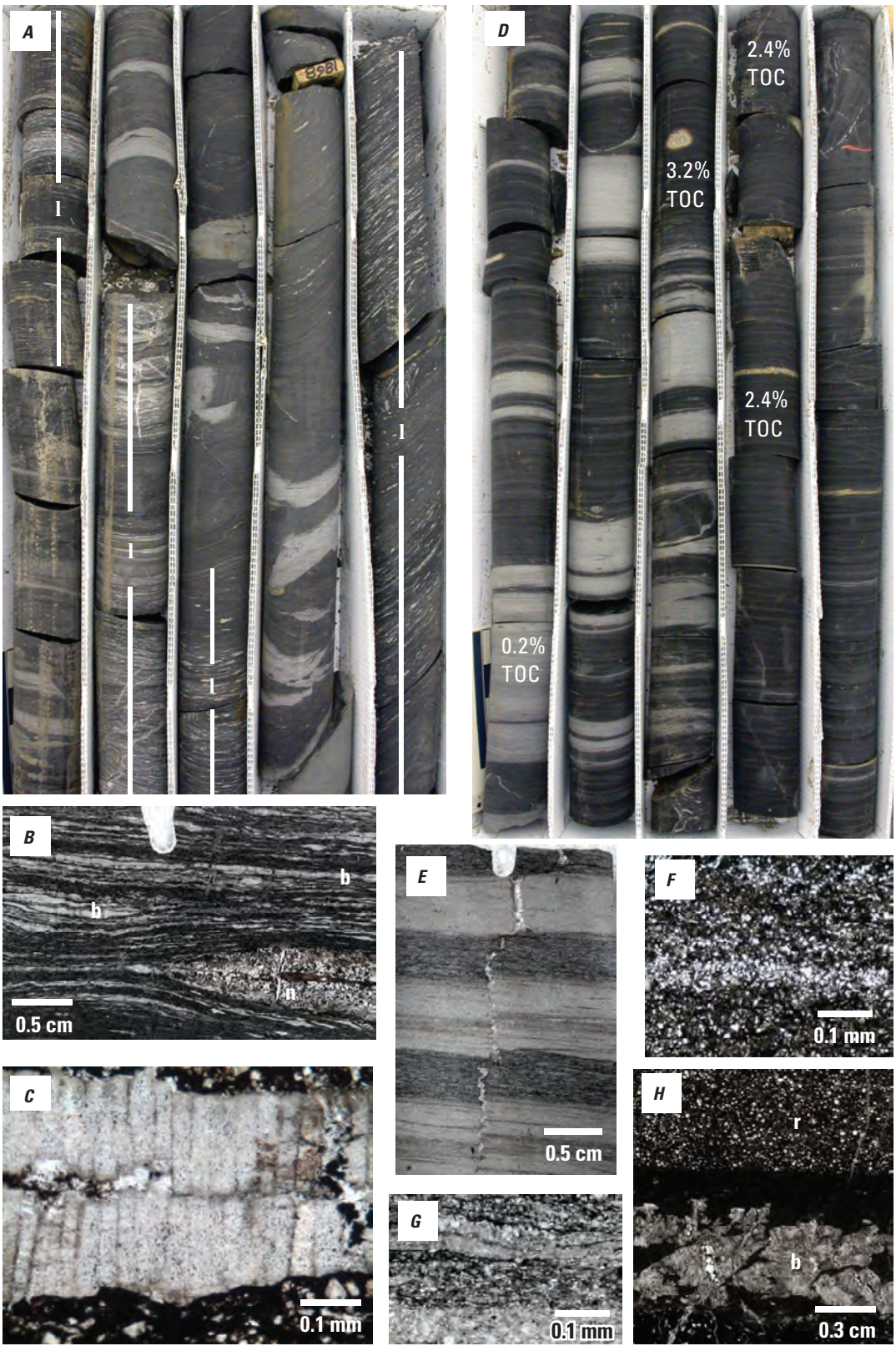

Figure 7. Photographs showing lithologic features of shale member of Otuk Formation in diamond-drill hole (DDH) 927. *A*, *D*, core photographs; *B*, *E*, *H*, thin section scans; *C*, *F*, *G*, photomicrographs. *A*, Black to pale gray silty shale contains limy intervals (l) rich in calcareous shell debris; core from 1,860.5 to 1,870.5 feet (ft) (top to left). *B*, *C*, Shells are mainly prismatic bivalves (b) that are likely *Claraia* sp.; cherty, phosphatic(?) nodules (n) occur locally; 1,862 ft. *D*, Silty shale ranges from black and organic-rich to pale gray and organic-poor; core from 1,850.5 to 1,860.5 ft (top to left). *E*–*G*. Silty to sandy layers contain parallel- and cross-laminae (*E*; 1,846 ft); some are rich in quartz (*F*; 1,866 ft), others in dolomite (*G*; 1,846 ft). *H*, Radiolarian-rich shale (r) above silty shale with lens of barite crystals (b); 1,793 ft. %, percent; TOC, total organic carbon. cm, centimeter; mm, millimeter.

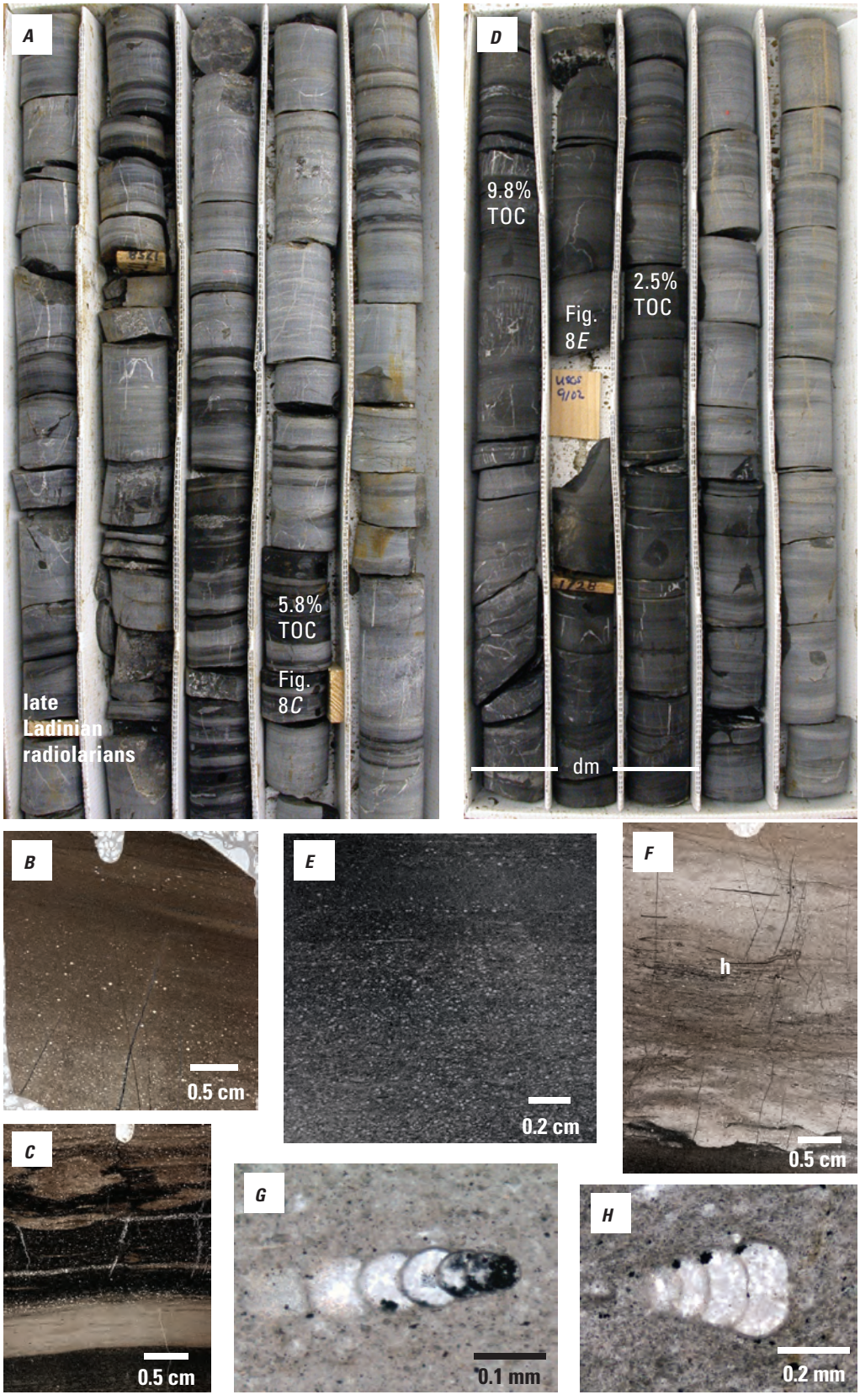

Figure 8. Photographs of lithologic features of chert member of Otuk Formation in diamond-drill hole (DDH) 927. *A*, *D*, core photographs; *B*,*C*, *E*, *F*, thin section scans; *G*, *H*, photomicrographs. *A*–*C*, Lower part of member: *A*, Gray chert with interbeds of dark, organic-rich, silty shale; core from 1,755.5 to 1,765 feet (ft) (top to left). *B*, Radiolarian chert (early to middle Ladinian) grades upward into shale; 1,774 ft. *C*, Interlayered, partly bioturbated, light and dark silty shale with locally abundant radiolarians; 1,760.8 ft. *D*–*H*, Upper part of member: *D*, Dark marker horizon (dm) overlies medium gray chert that makes up most of the chert member; core from 1,725 to 1,735 ft (top to left). *E*, Calcitized radiolarite from marker horizon; 1,728.3 ft. *F*, Partly bioturbated calcareous mudstone with halobiid bivalve fragments (h) from upper horizon; 1,720.7 ft. *G*, *H*, Calcareous foraminifers (possible members of the Lagenidae family; K. Bird, written commun., 2012) in upper horizon; 1,720–1,721 ft. %, percent; TOC, total organic carbon; cm, centimeter.

closer to the thickness of ~15-20 m reported for this interval in the Wolverine Creek plate by Young (2004).

In both drill holes, the lower part of the limestone member (figs. 4, 6) is mostly light gray lime mudstone to sparsely bioclastic wackestone variously replaced by chert and/or dolomite, and locally diluted by clay (fig. 9*A*, *B*). Halobiid and/or monotid flat clam fragments are sparse to common and in places they form coquinoid concentrations (fig. 9*B*). Radiolarians are also locally abundant but generally poorly preserved and replaced by carbonate.

In DDH 927, the lime mudstone-dominated interval is overlain by ~10.5 m (34.5 ft) of mostly light to medium gray radiolarian chert, locally shaly, with a layer ~1.2 m thick of blocky, brownish-black mudstone near the middle and ~30 cm of dolomitic lime mudstone at the top (figs. 6, 9*C*, *D*). Gray to black shale, with TOC values as much as 3.4 weight percent, forms <0.5- to 6-cm-thick interlayers in the chert (figs. 6, 9*C*, *D*, table A1). No bivalve fragments or foraminifers were seen in this interval; the carbonate mudstone contains abundant radiolarians (replaced by carbonate and pyrite) and a few phosphatic bioclasts.

The uppermost part of the limestone member in DDH 927 (dc, fig. 6) is mainly dark gray chert with thin interlayers of dark gray to black shale. Radiolarians occur throughout this interval and in places form size-graded layers capped by shale (fig. 9*E*); some of these layers also contain detrital grains such as quartz and feldspar silt, phosphate(?), and dark mudstone clasts as much as 4 mm long. Bivalve fragments and foraminifers are absent.

The overall stratigraphy of the limestone member in DDH 1110 is similar to that described above for DDH 927 (fig. 4). An interval of dolomitic lime mudstone that contains locally abundant flat clam fragments and calcitized radiolarians is overlain by radiolarian chert grading to siliceous mudstone. Shaly interlayers occur throughout the member and are mostly light gray with low TOC values (≤0.2 weight percent) in the limy interval and dark gray to black with as much as 3.8 weight percent TOC in the cherty interval (fig. 4, table A1). Thin layers and lenses of silt to fine sand, made up mostly of quartz, feldspar, carbonate, and fine-grained lithic clasts, occur locally in both intervals; one sandy layer near the middle of the cherty interval contains outsize mud clasts (as much as 2 mm long), radiolarians, phosphatic(?) grains, and detrital quartz silt to very fine sand.

Kingak(?) Shale

An interval of black, noncalcareous mudstone at least 35 m (115 ft) thick that overlies the limestone member of the Otuk Formation in DDHs 927 and 1110 (figs. 4, 10) was provisionally assigned to the Kingak(?) Shale by Young (2004) and Dumoulin and White (2005). The lower contact of the mudstone in both drill holes is conformable; the upper contact is a readily identifiable fault that is overlain by folded chert (Otuk Formation?) and then mélange in DDH 927 and by a mélange zone in DDH 1110. The Kingak Shale (Jurassic-Lower Cretaceous) crops out in the northeastern Brooks Range, is widely present in the subsurface beneath the North Slope, and has been recognized in the structurally lowest level of the EMA in the western and central Brooks Range (Magoon and Bird, 1988; Young, 2004; Dumoulin and White, 2005). It consists of dark shale and lesser siltstone and ranges from 17 to >1,000 m in thickness. The lower part of the Kingak correlates with the Blankenship Member of the Otuk, a distinctive organic-rich shale <20 m thick (Mull and others, 1982; Bodnar, 1984) that occurs discontinuously in higher plates of the EMA (Young, 2004).

Fissile oil shale and chert are characteristic of the Blankenship Member (Mull and others, 1982), but they are absent from the Kingak(?) Shale in the Anarraaq area (fig. 2). The mudstone in DDHs 927 and 1110 is grayish and brownish black to black, with subtle, millimeter-thick color laminae partly disrupted by bioturbation and soft-sediment folding (fig. 10*A*–*C*). Lenses and irregular blebs of pyrite as large as 1 cm in diameter, some of which are likely pyritized burrows, are scattered throughout the section. Most Kingak(?) samples in both drill holes contain trace to minor disseminated silt (mainly quartz and lesser feldspar) and a few contain minor silt- to sand-sized carbonate rhombs. Locally, silt is concentrated into lenses and laminae (fig 10*C*).

Kingak(?) Shale in the Anarraaq drill holes is relatively organic rich (fig. 4, table A1). TOC values of 1.3 to 3.7 weight percent (mean 2.1) were obtained from 11 representative samples taken through the section in DDH 927; 11 similarly selected samples from DDH 1110 had values of 2.1 to 6.5 weight percent (mean 3.4). These values are slightly higher than those from the Kingak in North Slope wells and in the northeastern Brooks Range, which range from 0.5 to 3 weight percent (Magoon and others, 1987; Magoon and Bird, 1988), but less than values typical of the Blankenship Member, which average 6.8 weight percent in the central Brooks Range (Bodnar, 1984).

A paleosol horizon occurs near the top of the Kingak(?) Shale in DDH 1110 (Dumoulin and White, 2005). A 3-cm-thick layer of black mudstone contains abundant magnesian siderite spherules that are 100 to 500 µm in diameter with an oxidized rim (fig. 10*D*), small dolomite rhombs ~20 µm in diameter, and small pyrite grains. The mudstone matrix is characterized by bimasepic to lattisepic fabric and roots indicative of pedogenesis (Dumoulin and White, 2005).

Age

Radiolarians and flat clam fragments constrain the age of the Otuk Formation in DDH 927 and 1110. No age data have been obtained from either the Siksikpuk Formation or the Kingak(?) Shale in these drill holes, but regional correlations limit the ages of these units.

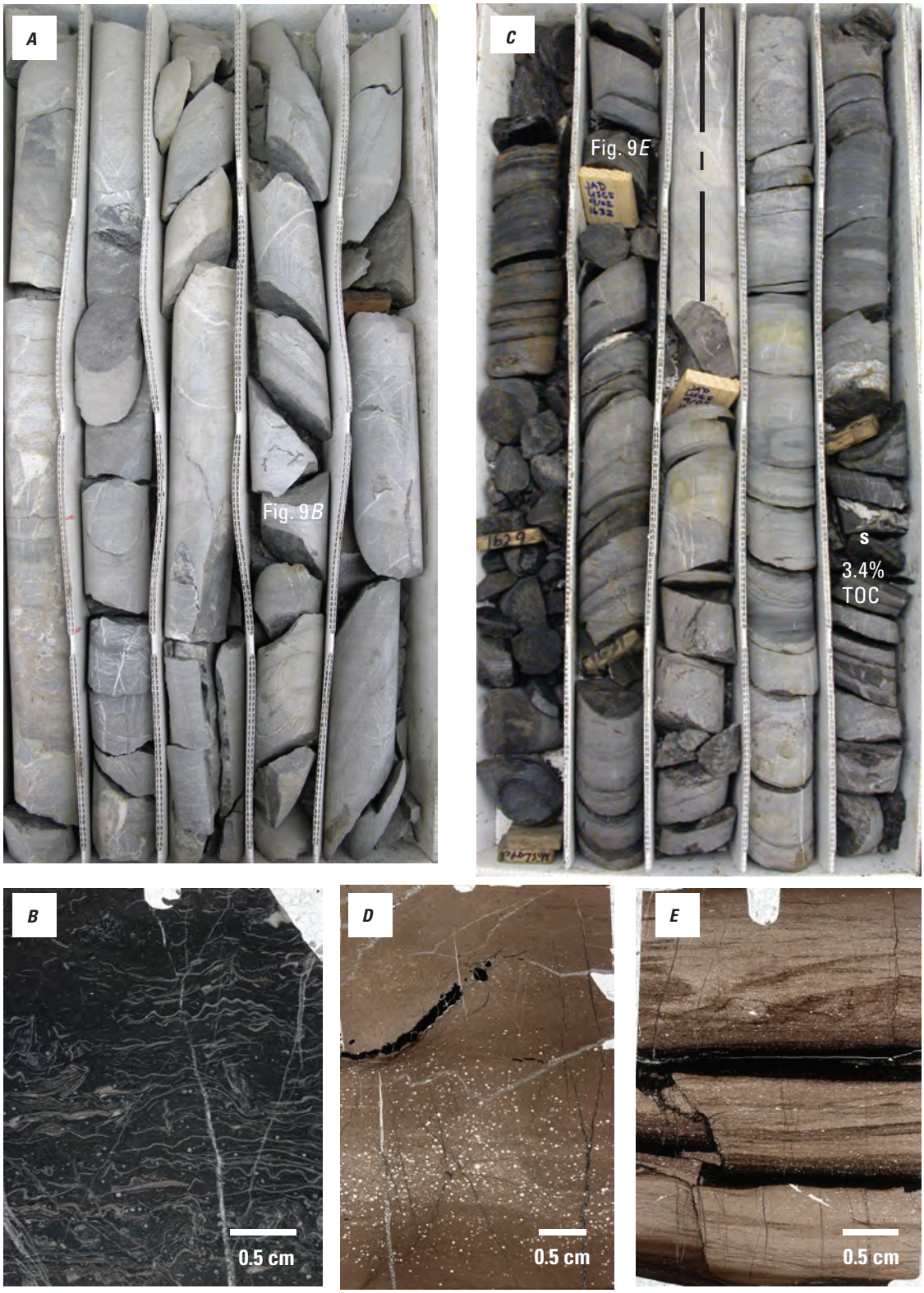

Figure 9. Photographs of lithologic features of limestone member of Otuk Formation in diamond-drill hole (DDH) 927. *A*, *C*, core photographs; *B*, *D*, *E*, thin section scans. *A*, *B*, Lower part of member consists mainly of lime mudstone to wackestone (*A*) with local concentrations of monotid bivalves (*B*; 1,682 feet, ft); core from 1,676 to 1,685.5 ft (top to left). *C*–*E*, Chert dominates the upper part of the member, with subordinate limy (l) and shaly (s) intervals (*C*); core from 1,628 to 1,638 ft (top to left). Radiolarians form crudely graded layers capped by shale and are of late Norian age in *D* (1,666 ft) and early Rhaetian age in *E* (1,632 ft). %, percent; TOC, total organic carbon; cm, centimeter.

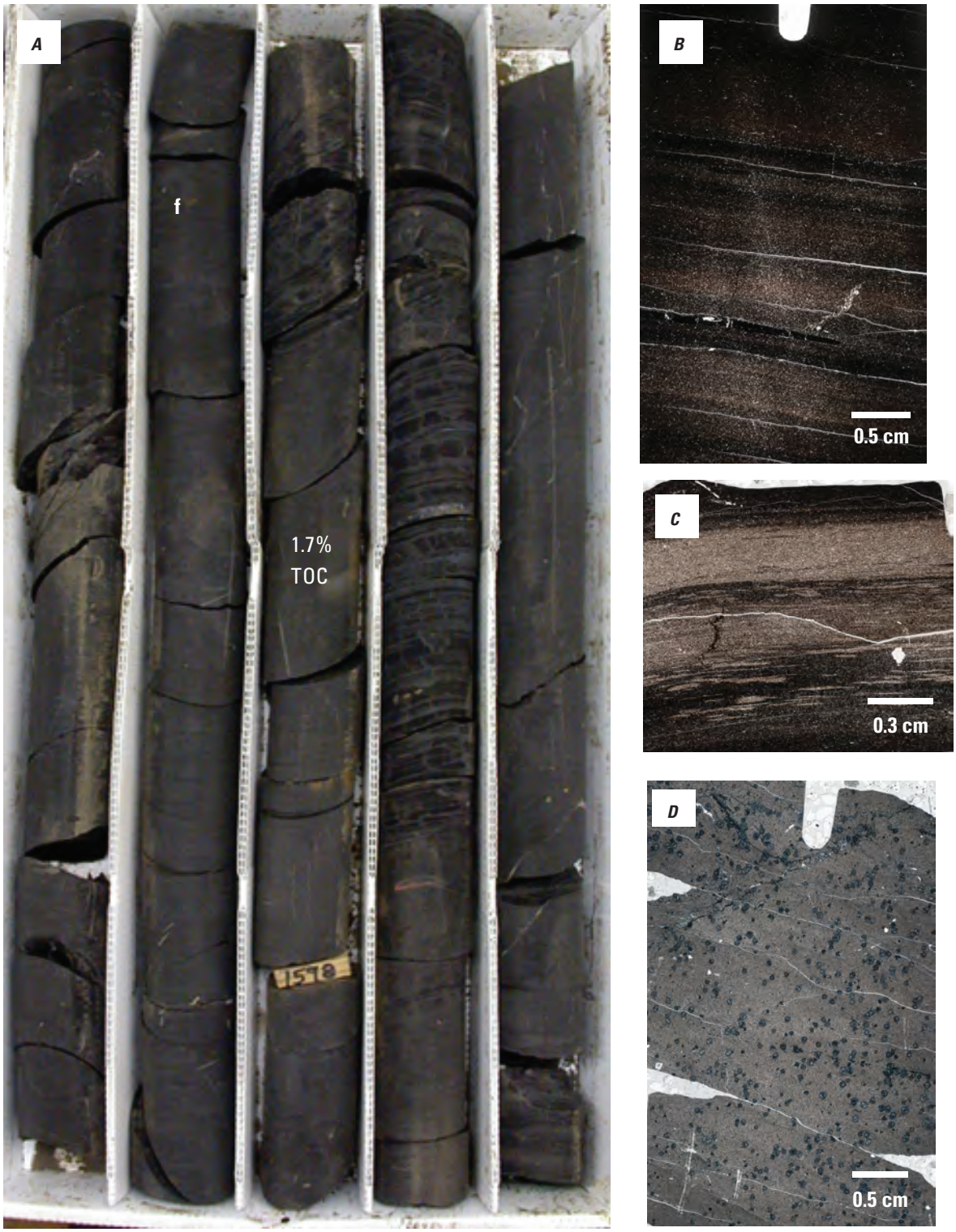

Figure 10. Photographs of Lithologic features of Kingak(?) Shale in diamond-drill holes (DDH) 927 (*A*–*C*) and 1110 (*D*). A, core photograph; *B*–*D*, thin section scans: *A*, *B*, Typical dark mudstone; TOC values range from 1.3 to 6.5 weight percent (fig. 4, table A1). Core from 1,594 to 1,605 feet (ft) (top to left); *B* from 1,600.8 ft. *C*, Thin partly bioturbated silty interval; 1,538 ft. *D*, Spherules of magnesian siderite in silty claystone paleosol near top of Kingak(?); 1,937 ft. %, percent; TOC, total organic carbon; cm, centimeter.

Siksikpuk Formation

Fossils indicate a Pennsylvanian-Permian age for the Siksikpuk Formation in the western Brooks Range (see discussion and references in Dumoulin and others, 2006). The only fossils seen in the upper subunit of the Siksikpuk in DDH 927 were agglutinated foraminifers (fig. 5*A*, *B*) that have not been dated. Radiolarians occur in a thin section of black shale from the transitional subunit (fig. 4), but a sample processed for radiolarians from this horizon was barren (table 1); the muddy matrix was difficult to disaggregate.

Definitively dated fossils younger than Middle Permian (Guadalupian) have not been reported from the Siksikpuk Formation regionally, and contact of the Siksikpuk with the overlying Otuk Formation has been interpreted as a disconformity, particularly in the central Brooks Range (for example, Bodnar, 1984). However, the transition between the Siksikpuk and the Otuk in DDH 927, as preserved in the transitional subunit of the Siksikpuk, is gradational and interbedded and thus appears to be conformable. Isotopic data, discussed below, support this interpretation.

Otuk Formation

Fossils indicate that the Otuk Formation in DDH 927 ranges from Early Triassic (early Smithian or older) to latest Triassic (late Rhaetian) in age. Radiolarians obtained from the limestone member of the Otuk in DDH 1110 provide additional ages from this subunit that agree well with the ages from DDH 927 (table 1).

Shale Member

Pelecypod debris suggests an age of Early Triassic for the lower part of the shale member in DDH 927. Limy intervals ~2.4 and 5.5 m (6 and 15 ft) above the base of the member (fig. 6) contain bivalve fragments made of prismatic calcite (fig. 7*B*, *C*) that are most likely derived from the flat clam *Claraia* sp. (T. Waller, U.S. National Museum, written communs., 2009, 2011). *Claraia* has long been recognized as a zonal taxon for the Early Triassic (McRoberts, 2010), and it has been found in Triassic rocks of northeastern Alaska. *Claraia stachei* occurs ~15 m above the base of the Kavik Member of the Ivishak Formation at its type locality in the northeastern Brooks Range, along with the ammonite *Ophiceras commune*; the fauna is early Early Triassic (earliest Griesbachian) (Detterman and others, 1975; fig. 3 in McRoberts, 2010). Definitive species assignment for *Claraia* cannot be made using thin sections, but details of internal shell texture seen in the samples from DDH 927 match well with those of *Claraia* cf. *stachei* illustrated by Boyd and Newell (1976). *Claraia* is absent from rocks of Spathian (latest Early Triassic) age, and few species persist beyond the early Smithian (early Olenekian; middle Early Triassic; Hallam, 1996; McRoberts, 2010). Thus, the occurrence of probable *Claraia* sp. fragments near the base of the shale member in DDH 927 suggests an age of Griesbachian to early Smithian for these beds.

Radiolarians were seen in thin sections from four levels in the shale member (fig. 6): in the higher of two levels that contain abundant bivalve fragments (?*Claraia* sp.) and at three horizons in the upper third of the unit. A sample from the lowest of these three horizons was barren (table 1); like the sample from the transitional unit of the Siksikpuk Formation discussed above, the muddy matrix proved difficult to disaggregate. Processing additional samples for radiolarians may yield more information on the age of this subunit in the future. Isotopic data (discussed below) suggest that the upper part of the shale member in DDH 927 is early Middle Triassic (Anisian); Bodnar (1984) reported an Anisian age for the upper part of the shale member in the central Brooks Range.

Chert Member

Radiolarians indicate that the chert member ranges from early Middle to Late Triassic in age. Four horizons yielded tightly dated radiolarian faunas; three additional samples produced less diagnostic fragments (fig. 6, table 1). An Anisian (early Middle Triassic) fauna was recovered from light to medium gray chert, 1 m (3.4 ft) above the base of the member. Similar rocks, ~4.5, 10, and 11 m (15, 33, and 37 ft) above the base, produced assemblages of probable early to mid-Ladinian, late Ladinian, and late Ladinian-early Carnian age, respectively. The age of the upper part of the chert member is less well constrained. Light gray argillaceous chert just below the base of the dark marker horizon produced only a few casts and molds that could not be dated, and lime mudstone near the top of the upper horizon yielded a poorly preserved fauna of Late Triassic (?Carnian-late middle Norian) age. Calcareous foraminifers and conodonts found in the upper horizon have not been dated; K.J. Bird (written commun., 2012) suggested that the foraminifers in figure 8*G* and *H* may be members of the long-ranging Lagenidae family (see Tappan, 1951). Young (2004) reported an age of Carnian or Norian for the dark marker horizon in the Red Dog plate.

Limestone Member

Radiolarians also constrain the age of the limestone member in DDHs 927 and 1110 (fig. 6, table 1), and integrating data from the two drill holes indicates an age of late middle or slightly older Norian through late Rhaetian (middle Late through latest Late Triassic). The lower, predominantly limy part of the unit contains flat clam fragments and is Norian, likely middle to late Norian, whereas the upper quarter of the member is mainly chert, lacks flat clams, and is early to late Rhaetian. Two samples taken for conodonts from the limy part of the unit (one each from DDHs 927 and 1110) were barren (Dumoulin and others, 2006).

Radiolarian faunas of definitively Rhaetian age have not previously been reported from the Otuk Formation. This may,

Table 1. Radiolarian samples from the Siksikpuk and Otuk Formations, diamond-drill holes (DDHs) 927 and 1110.

[USGS, U.S. Geological Survey]

Sample no. [USGS collection no.]	Unit [subunit]	Radiolarian fauna	Age
927-1885 [USGS DR 2534]	Siksikpuk Formation [transitional subunit]	Barren, nothing but black, recrystallized shale fragments found in the acid residues.	Unknown
927-1817.2 [USGS DR 2527]	Otuk Formation [shale member]	Barren, nothing but black, recrystallized shale fragments found in the acid residues.	Unknown
927-1786.5 [USGS DR 2528]	Otuk Formation [chert member]	*Pantanellium* ? *virgeum* Sashida *Spongostephanidium longispinosum* Sashida *Protopsium* sp. (abundant forms) No *Triassocampe* sp. found	early Middle Triassic (Anisian); *Hozmadia ozawai* Zone of Ohtaka and others (1998).
927-1778.4 [USGS DR 2536]	Otuk Formation [chert member]	Spine fragments of ?*Pseudostylosphaera* sp.	?Middle Triassic
927-1774 [USGS DR 2530]	Otuk Formation [chert member]	*Muelleritortis cochleata tumidospina* Kozur *Pseudostylosphaera coccostyla coccostyla* (Rüst) *Pseudostylospharea helicata* (Nakaseko and Nishimura) *Pseudostylosphaera japonica* (Nakaseko and Nishimura) *Triassocampe* sp.	Middle Triassic (Ladinian; probably early to mid-Ladinian); *Pseudostylosphaera helicata* assemblage of Sashida and others (1993).
927-1755.6 [USGS DR 2535]	Otuk Formation [chert member]	*Muelleritortis cochleata tumidospina* Kozur *Muelleritortis* sp. *Pseudostylosphaera coccostyla coccostyla* (Rüst) *Pseudostylosphaera* sp. aff. *Ps. goestlingensis* (Kozur and Mostler) *Pseudostylosphaera nazarovi* (Kozur and Mostler) *Triassocampe* sp. (rare) Other poorly preserved, unidentifiable nassellarians.	Middle Triassic (Ladinian, probably late Ladinian); *Cryptostephanidium* sp. assemblage of Sashida and others (1993); Zones TR 3A and TR 3B of Sugiyama (1997).
927-1752 [USGS DR 2519]	Otuk Formation [chert member]	*Muelleritortis cochleata cochleata* (Nakaseko and Nishimura) *Paronaella* sp. aff. *P. fragilis* Kozur and Mostler *Pseudostylosphaera compacta* (Nakaseko and Nishimura) *Pseudostylosphaera hellenica* (DeWever) *Pseudostylosphaera japonica* (Nakaseko and Nishimura) *Tritortis* sp.	late Middle to early Late Triassic (late Ladinian to early Carnian).
927-1732 [USGS DR 2533]	Otuk Formation [chert member]	A few poorly preserved radiolarian casts and molds.	Unknown

Table 1. Radiolarian samples from the Siksikpuk and Otuk Formations, diamond-drill holes (DDHs) 927 and 1110.—Continued

[USGS, U.S. Geological Survey]

Sample no. [USGS collection no.]	Unit [subunit]	Radiolarian fauna	Age
927-1720 [USGS DR 2540]	Otuk Formation [chert member]	All radiolarians very poorly preserved. One isolated spine which could belong to the radiolarian family, Capnuchosphaeridae DeWever, emended Blome, 1983. A few conodont fragments.	Late Triassic (?Carnian to late middle Norian).
927-1666 [USGS DR 2541]	Otuk Formation [limestone member]	?*Betraccium* sp. *Canoptum* sp. *Capnuchosphaera* sp. *Livarella* sp. aff. *L. valida* Yoshida *Pantanellium* sp. aff. *P. fosteri* Pessagno and Blome *Sarla* sp.	Late Triassic (late Norian); probably *Betraccium deweveri* Zone in Carter (1993) and Yeh (1992).
927-1632 [USGS DR 2532]	Otuk Formation [limestone member]	*Canutus*? *ingrahamensis* Carter *Canutus*? *beehivensis* Carter ?*Canutus* sp. *Pantanellium* sp. aff. *P. kungaense* Pessagno and Blome *Proparvicingula moniliformis* Carter (some displaying long horns)	Late Triassic (early Rhaetian; *Proparvicingula moniliformis* Zone of Carter, 1993).
927-1618.5 [USGS DR 2538]	Otuk Formation [limestone member]	*Citriduma asteroides* Carter *Canutus*? *beehivensis* Carter *Canutus*? *ingrahamensis* Carter *Globolaxtorum tozeri* Carter *Globolaxtorum cristatum* Carter *Laxtorum* sp. aff. *L. kulense* Blome *Orbiculiforma multibrachiata* Carter *Proparvicingula moniliformis* Carter	Late Triassic (late Rhaetian; *Globolaxtorum tozeri* Zone of Carter, 1993).
1110-2047.2 [USGS DR 2529]	Otuk Formation [limestone member]	Black casts and molds of radiolarians(?).	Unknown
1110-2067.5 [USGS DR 2537]	Otuk Formation [limestone member]	*Canutus* sp. *Laxtorum* sp.	Late Triassic (?Rhaetian)
1110-2103.3 [USGS DR 2539]	Otuk Formation [limestone member]	*Canoptum* sp. aff. *C. poissoni* Pessagno *Canoptum* sp. *Capnuchosphaera* sp. ?*Ferresium* sp. *Livarella* sp. *Pantanellium* sp. *Podobursa*-like nassellarian, figured in Pessagno and others (1979)	Late Triassic (late middle Norian; *Pantanellium silberlingi* Zone of Pessagno, 1979, and emended by Blome, 1984).

at least in part, reflect the fact that most studies of Otuk radiolarians (for example, Blome and others, 1988) were carried out before the work of Carter (1993), who was the first to propose radiolarian zones for the Rhaetian in North America. However, regional correlations suggest that the cherty interval at the top of the Otuk that has yielded Rhaetian radiolarians in the Red Dog District may be missing or represented by a different facies to the east; this suggestion is further discussed below.

Kingak(?) Shale

The Kingak Shale is of Jurassic through Early Cretaceous age in northern Alaska (Magoon and Bird, 1988). No age-diagnostic fossils have been found in the Kingak(?) Shale in the Anarraaq area, but stratigraphic relations suggest an Early Jurassic (and younger?) age. Basal contact of the Kingak(?) with the limestone member of the Otuk Formation appears conformable and latest Triassic (late Rhaetian) radiolarians occur ~2 m (7 ft) below the contact in DDH 927 (fig. 4, table 1). The paleosol horizon near the top of the Kingak(?) in DDH 1110 (Dumoulin and White, 2005) may correlate with exposure surfaces in Lower Jurassic strata of Kingak sections penetrated by wells on the North Slope (Houseknecht, 2001; Houseknecht and Bird, 2004).

Depositional Setting

The Otuk Formation is generally thought to represent condensed, distal deposition on a broad, gently sloping marine shelf remote from clastic source areas (Bodnar, 1984; Young, 2004). Kelly and others (2007) suggested mainly outer shelf to basinal settings for the section at Tiglukpuk Creek (fig. 1), and they interpreted intervals dominated by limestone, shale, and chert, respectively, as having formed in successively deeper water. Bodnar (1984) inferred that the shale through limestone members of the Otuk in the central Brooks Range formed during a single transgressive-regressive cycle, whereas Kelly and others (2007) proposed that most of the Otuk at Tiglukpuk Creek (upper shale member through limestone member) was deposited during three third-order cycles of marine transgression and regression. Ichnofabric and geochemical data suggest that the Tiglukpuk Creek Otuk section accumulated mainly in oxic and dysoxic environments, with the most organic-rich facies deposited in low-oxygen settings during transgression (Kelly and others, 2007).

Lithologic and biotic data from the Otuk Formation and overlying Kingak(?) Shale in the Anarraaq area support much of the interpretation outlined above, and suggest deposition mainly in oxic to dysoxic, outer shelf and deeper settings below the carbonate compensation depth (CCD). Limy layers, with abundant calcareous fossil fragments and (or) fine-grained carbonate matrix, occur mainly in the lower parts of the shale and limestone members and imply that these intervals were deposited above the CCD. These observations, however, provide little constraint on absolute water depths, because the CCD varies greatly in space and time. The CCD is generally at ~3,000 to 5,000 m depth in modern oceans, but it decreases sharply adjacent to continental margins and may have been considerably shallower before mid-Mesozoic proliferation of calcareous plankton (Berger and Winterer, 1974).

Dark, organic-rich shale that makes up much of the lower half of the Otuk Formation and virtually all of the Kingak(?) Shale in DDH 927 is interpreted here as the predominant sediment type on the Otuk shelf. Paleontologic and geochemical data suggest that similar facies at Tiglukpuk Creek formed in poorly oxygenated settings (Bodnar, 1984; Kelly and others, 2007). Thin layers of light-colored, silty shale to fine-grained sandstone found sporadically through the Otuk in DDH 927 are likely distal turbidites, based on locally well-developed sedimentary structures such as normal size grading and parallel and cross laminae (fig. 7*E*); some radiolarite layers appear graded and may also be turbidites (figs. 8*C*, 9*E*). Siliciclastic detritus may have derived from eastern and (or) western sources (in present-day coordinates); this issue is considered further below.

Radiolarian chert, most abundant in the upper parts of the chert and limestone members of the Otuk Formation at Anarraaq, may have formed in the deepest water settings, as suggested by previous authors (for example, Kelly and others, 2007). Oceanographic factors may also have affected distribution of this facies. Phosphatic intervals occur through much of the Shublik Formation in outcrop and subsurface and are thought to have accumulated in response to a marine upwelling system that was initiated in the late Middle Triassic and persisted through the Late Triassic (Parrish and others, 2001; Kelly and others, 2007). Concentrations of radiolarians in the Otuk appear analogous to modern plankton accumulations in high-productivity upwelling zones; thus, thick intervals of radiolarian chert could indicate times of more intense upwelling rather than specific water depths.

Much of the Otuk Formation and Kingak(?) Shale section in DDH 927 is partly bioturbated (for example, fig. 8*F*), indicating that bottom waters were not anoxic. However, fossils are predominantly pelagic (radiolarians) or opportunistic benthic forms suited to oxygen-deficient conditions (claraid, halobiid, and monotid bivalves; McRoberts, 2010), suggesting dysoxia was prevalent. The abundance of organic-rich shale is consistent with this interpretation, but it could also be due, at least in part, to the sediment-starved setting, which minimized dilution of organic matter by other detritus.

In summary, the Otuk Formation and Kingak(?) Shale in the Anarraaq area accumulated on the outer part of a broad marine shelf. Lithofacies and biofacies suggest dysoxic conditions were common, and were likely caused, at least in part, by development of an oxygen-minimum zone associated with a marine upwelling system (Parrish and others, 2001; Kelly and others, 2007). Whole-rock geochemical analyses of the Anarrraaq section, the focus of a future study, should yield additional insights into oxygenation levels during deposition. Alternation of limestone, shale, and chert throughout the DDH

927 section likely reflects both eustatic and oceanographic factors. Limy intervals rich in bivalve fragments formed in the shallowest settings and are found in the lower shale, upper chert, and lower limestone members (fig. 6). This distribution supports the contention of Kelly and others (2007) that the Otuk records more than one transgressive-regressive cycle. Episodic influx of silt and fine sand, largely as distal turbidites, occurred throughout deposition of the Anarraaq section but was most pronounced during Early, Middle, and latest Triassic (Rhaetian) times.

Correlations

Detailed lithofacies of the Otuk Formation vary in concert with changes in structural and stratigraphic position (for example, Mull and others, 1982; Bodnar, 1984; Young, 2004). In this section, we compare the Otuk succession in the Wolverine Creek plate of the EMA to that found in several higher structural levels in the Red Dog area (figs. 2, 11). We then compare our section with Otuk successions that have been described to the west (Lisburne Peninsula) and east (Tigluk-puk Creek; fig. 1).

Red Dog District

Detailed information on facies of the Otuk Formation in the Red Dog District come mainly from drill-hole penetrations of this unit in the Red Dog plate of the EMA, which structurally overlies the Wolverine Creek plate (Young, 2004). In addition, radiolarian faunas and some facies data are available from a section in the PCA at Punupkahkroak Mountain (Blome and others, 1988).

EMA, Red Dog Plate

We examined the Otuk Formation in the Red Dog plate of the EMA, in drill core from DDH 1150C in the southern part of the Anarraaq deposit (fig. 2). No age control is available for this section. The chert member may be structurally thickened, and its upper contact is a fault. Contact between the shale member and the underlying Siksikpuk Formation is gradational. Both shale and chert members in DDH 1150C are generally similar to those in DDH 927; they differ mainly in containing few calcareous intervals but many horizons that are rich in barite. Bivalve fragments were not observed in any of our samples from DDH 1150C. Barite occurs as bladed crystals, commonly intergrown with pyrite or dolomite. The limestone member is typically thin (a few meters thick) or absent in the Red Dog plate; where present, it consists of cherty limestone and limy chert with rare to abundant monotid pelecypods (Young, 2004). An exposure of the limestone member in the Red Dog plate ~4 km east of Anarraaq (loc. 66 in Dumoulin and others, 2006) contains rare monotids and radiolarians of late middle Norian (*Pantanellium silberlingi* Zone) age. The uppermost part of the Otuk in the Red Dog plate consists of 3 to 6 m of laminated black chert and shale. These strata were assigned to the Blankenship Member by Young (2004) but are undated and could be equivalent to the cherty (Rhaetian) upper part of the limestone member in DDH 927.

Picnic Creek Allochthon

Exposures of the Etivluk Group at Punupkahkroak Mountain, ~18 km west-southwest of Anarraaq (fig. 2), were previously considered part of the Ipnavik River Allochthon (Blome and others, 1988; Mayfield and others, 1990). More recent mapping (De Vera and others, 2004; Young, 2004) indicates that these strata are part of the PCA. Permian-Jurassic rocks in this allochthon are much chertier than coeval successions in the EMA; the Siksikpuk and Otuk Formations typically cannot be distinguished and are mapped as Etivluk Group undivided.

About 90 m of the upper Etivluk Group at Punupkahkroak Mountain was briefly described by Blome and others (1988). No beds equivalent to the Siksikpuk Formation were recognized here. The section is mostly thin-bedded, dark gray to olive-gray chert, with 10 m of interbedded chert and limestone near the top of the section (fig. 11). Radiolarians indicate that the lowest rocks are Ladinian or early Carnian to late Carnian, overlain by early Norian to late middle Norian strata. The limy part of the section is late middle to late Norian and contains *Monotis* sp. About 10 m of chert at the top of the section produced radiolarian faunas that are late Norian and Early Jurassic (Hettangian, Hettangian-Sinemurian, and late Pliensbachian-Toarcian).

Lisburne Peninsula

Several sections of the Otuk Formation have been briefly described from the Lisburne Peninsula ~125 km west of the Red Dog District (figs. 1, 2). Young (2004) considered these rocks parautochthonous, but Mayfield and others (1988) included them in the EMA. The most detailed lithofacies and faunal data are available (Blome and others, 1988) from two partial, overlapping sections in the northwestern part of the peninsula near Cape Lisburne (figs. 1, 2, 11). In the Ayugatak Creek section, the Otuk conformably overlies the Siksikpuk Formation. Shale and chert members of the Otuk here are each ~25 m thick and partly covered. The shale member consists of soft, black, sooty, calcareous shale that becomes more siliceous upward and contains the flat clam *Daonella* sp. near the top. Reddish-brown-weathering chert with shale partings makes up much of the chert member, with an interval of black sooty limestone and shale near the middle of the member that may be equivalent to the dark marker horizon in the Red Dog area. About 3 m of the limestone member—limestone beds with abundant monotid bivalves—form the upper part of the section, the top of which is truncated by Holocene erosion.

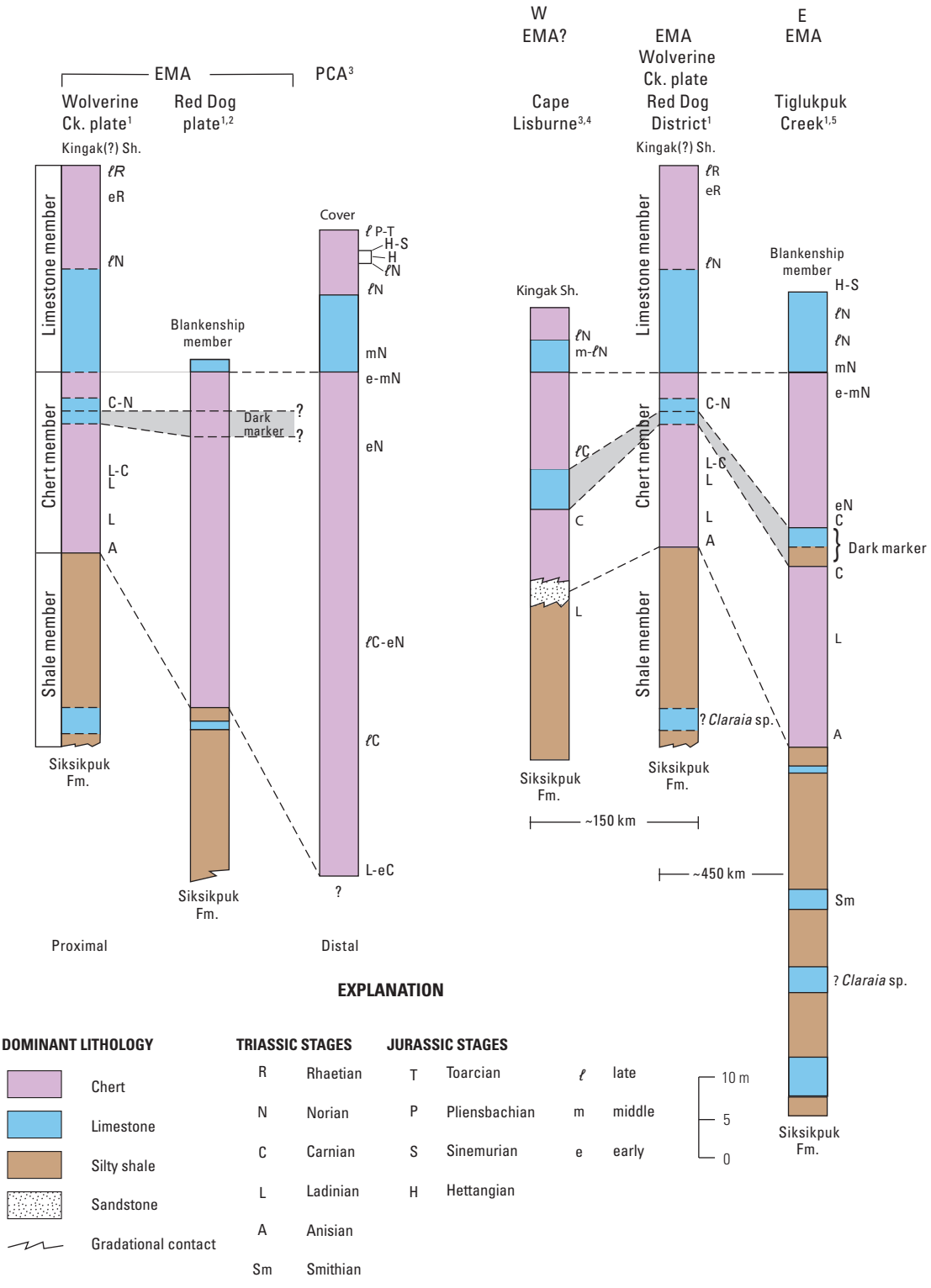

Figure 11. Diagram showing correlation of the Otuk Formation in the Wolverine Creek plate of the Endicott Mountains Allochthon (EMA) (diamond-drill hole, DDH, 927) with equivalent strata from higher structural levels in the Red Dog area (Red Dog plate of EMA, Picnic Creek Allochthon, PCA) and with EMA successions to the west and east. PCA section is at Punupkahkroak Mountain (fig. 2). Data sources: 1, this study; 2, Young (2004); 3, Blome and others (1988); 4, Moore and others (2002); 5, Bodnar (1984), Kelly (2004), Kelly and others (2007). Sh., shale; Ck., creek; km, kilometers.

About 15 km to the west at Noyalik Peak, more of the upper part of the Otuk Formation can be seen. This section begins with the chert member, which is ~15 m thick and made up of dark gray to black chert with thin shale interbeds. Limy layers appear near the top of the member, and increase in abundance upward. The limestone member is ~10 m thick. It consists of ~5 m of partially silicified limestone, with local wispy bedding and coquinoid concentrations of monotid bivalves, overlain by an equal thickness of interbedded shale and chert.

Detailed mapping by Moore and others (2002) indicated that as much as 5 m of sandstone occurs between the shale and chert members of the Otuk Formation in parts of northwestern Lisburne Peninsula. The sandstone may be a turbidite (T.E. Moore, U.S. Geological Survey, USGS, written commun., 2011); it is very fine to fine-grained and made up of quartz, lithic grains, and lesser feldspar. Lithic grains include argillite, chert, siltstone, granite, and carbonate (Moore and others, 2002).

Less is known about the Otuk Formation in the southern part of the Lisburne Peninsula, but its general stratigraphy appears similar to that seen in the north (Campbell, 1967; Blome and others, 1988). A chert-rich interval that lacks monotids also forms the uppermost part of the Otuk in this area; this cherty zone is as much as 10 to 13 m thick in several sections near Agate Rock (fig. 2).

Radiolarians and flat clams partly constrain the age of the Otuk Formation on the Lisburne Peninsula (Blome and others, 1988; fig. 11). *Daonella* sp. near the top of the shale member is late Anisian-middle Ladinian (McRoberts, 2010). The chert member is in part Carnian, and the monotid beds of the limestone member are middle and late Norian. Radiolarians from the lower part of the chert and shale interval at the top of the Otuk are also late Norian, but the uppermost beds of this interval have not been dated.

Central Brooks Range

Tiglukpuk Creek

The section of the Otuk Formation at Tiglukpuk Creek (fig. 1) is the most complete exposure of this unit in the central Brooks Range and has been investigated by a number of workers (Bodnar, 1984; Blome and others, 1988; Kelly and others, 2007; Whidden and others, 2012; this study). The Otuk here is ~120 m thick, overlies the Siksikpuk Formation, and underlies the Lower Cretaceous Okpikruak Formation. Bodnar (1984) interpreted the lower contact as a disconformity marked by a paleosol, and the upper contact as a fault. The shale member is ~50 m thick and consists of varicolored silty shale and siltstone with numerous limy and dolomitic interbeds. Prismatic bivalve fragments (?*Claraia* sp.) are found in some of the lower carbonate beds (this study), and *Peribositria mimer* of middle to late Smithian age (McRoberts, 2010) occurs slightly higher (Kelly and others, 2007). Chert and porcellanite make up much of the chert member, which is also ~50 m thick and contains subordinate interbeds of shale and carbonate. Conodonts (Bodnar, 1984) of Anisian age (Orchard, 2010) and Ladinian, Carnian, and early to middle Norian bivalves (Bodnar, 1984; Kelly and others, 2007) constrain the age of this member. More than 30 thin layers of yellow claystone, as much as a few centimeters thick, occur through both the shale and chert members and are interpreted as bentonites (M. Whalen, oral commun., 2011). About 12 m of light gray, locally cherty, monotid-bearing limestone, with interbeds of gray and rare black shale, makes up the limestone member; bivalves indicate an age of middle and late Norian (Bodnar, 1984; Kelly, 2004; Kelly and others, 2007; Whidden and others, 2012). These rocks are overlain by the Blankenship Member, here represented by ~9 m of thinly interbedded black shale and chert with Jurassic bivalves (Bodnar, 1984; Kelly and others, 2007).

Discussion

Regional correlations outlined above indicate that lithofacies in the Otuk Formation vary with both structural and geographic position (fig. 11). In the Red Dog District, the shale and chert members of the Otuk in the Wolverine Creek plate contain more limestone and less barite than equivalent strata in the structurally higher Red Dog plate of the EMA, and the limestone member in the Red Dog plate is thin or absent. In the PCA, which structurally overlies the EMA, rocks coeval with the Otuk (upper Etivluk Group) are mostly chert, with a monotid-bearing limy interval equivalent to the lower part of the limestone member in the Wolverine Creek section. Definitively Rhaetian radiolarians have not been recognized in the PCA, but they might be expected to be present just below the Early Jurassic faunas at the top of the Etivluk in this allochthon. A fauna collected near the top of the Etivluk Group in the PCA, ~ 40 km northeast of the Punupkahkroak Mountain section and ~32 northeast of Anarraaq, is of late Norian or Rhaetian age (loc. 33 in Dumoulin and others, 2006).

Lithofacies of the Otuk Formation also differ within the EMA from east to west. Both the shale and chert members in the Red Dog District contain less limestone than equivalent strata at Tiglukpuk Creek. Monotid-bearing beds in the limestone member in the Red Dog District are overlain by an interval of chert and shale that is partly of Rhaetian age. No such beds occur to the east but lithologically similar, as yet undated strata that could be coeval are seen at the top of the Otuk on the Lisburne Peninsula. Bentonitic claystones like those at Tiglukpuk were not seen in the Red Dog area, but silty layers with notable feldspar grains, found in the Otuk of both the Wolverine Creek and Red Dog plates, could reflect a tuffaceous component.

The lithologic differences summarized above are consistent with the interpretation that Triassic and Lower Jurassic facies become increasingly more distal in higher

structural positions (Young, 2004) and perhaps also from east to west (Bodnar, 1984). Limestone decreases and chert increases, both east (Tiglukpuk) to west (DDH 927) and structurally lower (Wolverine Creek plate of the EMA) to higher (PCA). The abundance of barite in the Otuk Formation in the Red Dog area, and particularly in the Red Dog plate, likely reflects local stratigraphy. World-class barite deposits in the underlying Lisburne Group in this area (for example, Johnson and others, 2004) would have provided a ready source of barium that could migrate upward and precipitate in overlying sediments (C.A. Johnson, written commun., 2011).

As noted above, the structural position of Triassic successions on the Lisburne Peninsula is uncertain (parauthochthonous or EMA). Lithofacies and faunal data from these sections are still too sketchy to provide a definitive comparison with those of the Red Dog District. One particularly intriguing open question is whether undated chert and shale at the top of the Otuk on the Lisburne Peninsula correlates with lithologically similar Rhaetian strata in DDH 927, and/or with Early Jurassic rocks at the top of the Etivluk Group in the PCA.

Silt and sand grains and layers in the Otuk Formation have generally been thought of as sourced from the northeast (for example Bodnar, 1984), where silty and sandy facies such as the Ivishak Formation (Lower Triassic), the siltstone member of the Shublik Formation (Middle Triassic), and the Karen Creek Sandstone (Rhaetian) accumulated through much of Triassic time. Most silt and sand in the Otuk in DDH 927 indeed occurs in strata equivalent in age to these units. The presence of a thick sandstone layer in the Otuk on the Lisburne Peninsula (Moore and others, 2002), however, complicates the interpretation of siliciclastic provenance. Detrital zircon ages from this sandstone have a probability distribution like those of Triassic turbidites of the Chukchi Peninsula, northeastern Russia, and distinctly different from that of a sample of the Ivishak Formation (Miller and others, 2006), implying that western and eastern sources contributed detritus to Triassic sediments in northern Alaska. Analysis of detrital zircons from siliciclastic-rich layers in the Otuk of the Red Dog District and the central Brooks Range would improve our understanding of Triassic provenance patterns.

Geochemistry of Organic Carbon

The stratigraphic variability of the concentration and stable isotopic composition of organic carbon in marine sediments can reveal important characteristics of the environments of sediment accumulation and the global carbon cycle. Changes in the global carbon cycle can lead to variations in the geochemistry of organic carbon, especially the stable isotopic composition, that can be correlated globally, providing markers that can be correlated with biostratigraphy and other lithostratigraphic variations (for example, Krull and others, 2004; Tanner, 2010). In this section we describe the variations in total organic carbon (TOC) and carbon isotopic composition of organic carbon ($\delta^{13}C_{org}$) in the Permian to Jurassic age strata in DDH 927 and Triassic to Jurassic age strata in DDH 1110. Analytical methods and a table of measured values are provided in the appendix.

TOC Measurements and Thermal Data

Total organic carbon (TOC) values of the Otuk Formation in DDHs 927 and 1110 (figs. 4, 6, table A1) are the first published from this unit in the western Brooks Range and, like those determined from equivalent strata in the central Brooks Range (Bodnar, 1984; Kelly and others, 2007), demonstrate that organic-rich shale with excellent potential as a hydrocarbon source rock is abundant and widely distributed through the unit. Shale containing >2 weight percent TOC occurs in all three members of the Otuk, as well as in the overlying Kingak(?) Shale. Limestone and chert were not analyzed for TOC in our study, which focused on determining the range of organic content in the mudrocks we encountered.

Organic-rich shale is most abundant in the lower half of the Otuk Formation in DDH 927. Dark gray to black silty shale with 1.3 to 6.9 weight percent TOC (mean, 3.8; n=11; fig. 6) makes up ~60 percent of the shale member and ~10 to 15 percent of the lower half of the chert member, and is interbedded in both members with light- to medium-gray silty shale that has 0.12 to 0.25 weight percent TOC (mean, 0.2; n=5). In the upper half of the Otuk, organic-rich shale is less common. More than half of the 2.4-m-thick dark marker horizon near the top of the chert member consists of black shale to mudstone with up to 9.8 weight percent TOC (fig. 6). Shale in the lower part of the limestone member is light gray and contains little TOC (≤0.2 weight percent; fig. 4), but dark gray shale with as much as 3.8 weight percent TOC forms about one fifth of the upper part of the member (figs. 4, 6).

Kingak(?) Shale overlying the Otuk Formation in DDHs 927 and 1110 is also organic rich. TOC values of 22 samples range from 1.3 to 6.5 weight percent (mean, 2.74), and three-quarters of the values are ≥2.

High TOC values have been found in several fault-bounded partial sections of the Otuk Formation from the Red Dog plate in the Anarraaq area. Samples of black silty shale from the shale member of the Otuk in DDHs 778 and 801 contain 7.4 and 9.5 weight percent TOC, respectively (J. Slack, USGS, written communs., 2001, 2005). In both sections, dark shale is interbedded with pale to medium gray shale, siltstone, and siliceous mudstone that has little TOC (0.15–0.17 weight percent; n = 2).

The range of TOC values in the Otuk Formation at Anarraaq is similar to that reported from coeval strata in the central Brooks Range, but the distribution of values through the unit differs in part. At Tiglukpuk Creek (fig. 1), as in DDH 927, much of the shale member contains ≥2 weight percent TOC, and values are highest (~3–7 weight percent) in the upper half of the member (Kelly and others, 2007). Bodnar (1984) documents similar TOC patterns in the shale member of Otuk

sections at Encampment Creek and Okpikruak River, 15 and 80 km west of Tiglukpuk. Black shale in the upper part of the chert member at Tiglukpuk Creek, like that in the dark marker horizon in DDH 927, is very organic rich with as much as 10.77 weight percent TOC (Kelly and others, 2007). But TOC values in the upper part of the Otuk in the central Brooks Range are higher than those of equivalent rocks at Anarraaq. Black shale in the limestone member contains as much as 8.55 weight percent TOC at Tiglukpuk Creek (Kelly and others, 2007) and 10.63 weight percent TOC at Otuk Creek in the Killik River quadrangle (Bodnar, 1984). TOC values as high as 8 to 13.9 weight percent occur in black shale of the Blankenship Member at Otuk Creek and several other sections sampled by Bodnar (1984) and Kelly and others (2007).

TOC values of the Shublik Formation are generally low in outcrop but higher in the subsurface (Kelly and others, 2007, and references therein). Carnian age organic-rich shale of the Shublik in the Phoenix #1 well off the north-central coast of Alaska (fig. 1; Robison and others, 1996; Blodgett and Bird, 2002) is broadly coeval with organic-rich shale in the dark marker horizon of the chert member in DDH 927.

Vitrinite reflectance (R_o) was measured by Weatherford Laboratories on two samples of black shale in order to assess the thermal maturity of the Otuk Formation in DDH 927. Both samples are organic rich and come from the chert member (927–1,730 ft, 5.0 weight percent TOC; 927–1,778 ft, 6.4 weight percent TOC). The R_o values of 2.45 and 2.47 percent, respectively, indicate that both samples are in the dry gas window. R_o data are consistent with thermal alteration index values of amorphous kerogen and with fluorescence data obtained from these samples. These thermal maturity parameters are in turn consistent with regional estimates based on conodont color alteration index values of 2.5 to 3.5 (Dumoulin and others, 2004, 2006). Amorphous kerogen is more abundant than terrestrial kerogen in both DDH 927 samples. Solid bitumen particles are common, suggesting that some liquid hydrocarbon has been generated from these rocks.

Carbon Isotopes

A suite of $\delta^{13}C_{org}$ data (n=38) from the upper Siksikpuk Formation through the Otuk Formation and into the Kingak(?) Shale in DDH 927 (fig. 12) shows a pattern of positive and negative carbon isotope excursions (CIEs) similar to those reported elsewhere in Triassic strata (Tanner, 2010, and references therein). The isotopic data, combined with sedimentologic and paleontologic information discussed above, suggest that the Otuk section in DDH 927 represents a largely complete, albeit condensed, record of Triassic sedimentation. As stated in the section on TOC measurements, geochemical sample collection focused on mudrocks, therefore, sample spacing was not uniform.

Permian-Triassic Boundary

A distinct negative excursion in $\delta^{13}C_{org}$ at the base of the Otuk Formation (carbon isotope excursion (CIE) 1, fig. 12) likely correlates with a pronounced excursion that marks the Permian-Triassic boundary at many localities worldwide. This excursion has been found in both $\delta^{13}C_{org}$ (organic) and $\delta^{13}C_{carb}$ (carbonate) from marine and terrestrial sediments at sites in the Tethyan and Neotethyan realms, regions bordering Panthalassa, and in South China (Tanner, 2010). The ubiquity and magnitude of this excursion have led to its use by many workers as a chemostratigraphic marker for the Permian-Triassic system boundary (Krull and others, 2004; Tanner, 2010); it is associated with a long-term offset to more negative carbon values across the system boundary (Retallack and Krull, 2006).

In DDH 927, the excursion extends from ~16 m (54 ft) below the top of the Siksikpuk Formation to ~3.2 m (10.5 ft) above the base of the Otuk Formation (fig. 12). The magnitude of the excursion is −7.5‰ (permil, or parts per thousand; from −23.8 to −31.3‰; table 2), which falls in the middle of the range of magnitudes reported by Retallack and Krull (2006) in their compilation of both the transient $\delta^{13}C$ excursion and the long-term offset of $\delta^{13}C$ across the Permian-Triassic boundary. These authors reported an average isotopic excursion at the system boundary, for organic carbon in both marine and nonmarine rocks, of −6.4±4.4‰ (n=30) with a range from −2.2 to −22.2‰; the average for marine rocks is −7.0±3.5‰ (n=14) with a range of −2.2 to −15‰ (table 2). The apparent long-term offset in average carbon values across the system boundary in DDH 927 is ~−5‰ (from ~−24‰ in the Permian to −29‰ in the Triassic), which falls in the −0.3 to −7.7‰ range for this parameter observed in marine and nonmarine rocks by Retallack and Krull (2006).

Both the long-term offset and the transient excursion in $\delta^{13}C_{org}$ at the Permian-Triassic boundary are greater at high latitudes (Retallack and Krull, 2006). Boundary excursion and long-term offset values in DDH 927 are most similar to those determined for marine organic carbon at two sites in Australia (Morante, 1996), in the Schuchert Dal Formation, Greenland (Twitchett and others, 2001), and in Festningen, Spitsbergen (Wignall and others, 1998), which have estimated paleolatitudes of −37±6°, -40±6°, +38±6°, and +46±6° respectively (table 2; Retallack and Krull, 2006). These compare well with paleolatitudes of ~+45–60° that have been proposed recently for northern Alaska during the Late Permian-Early Triassic (Scotese, 2001; Lawver and others, 2002; Kelly and others, 2007; Colpron and Nelson, 2009).

Lithologic data, faunal data, and regional correlations support the implication of the isotopic data that DDH 927 preserves a relatively complete Permian-Triassic boundary section. No age-diagnostic fossils have been found in the uppermost Siksikpuk Formation in the Red Dog District, but a conformable contact between the Sikisikpuk and the overlying Otuk Formation is suggested by the gradational, interbedded nature of this contact that is observed throughout the district

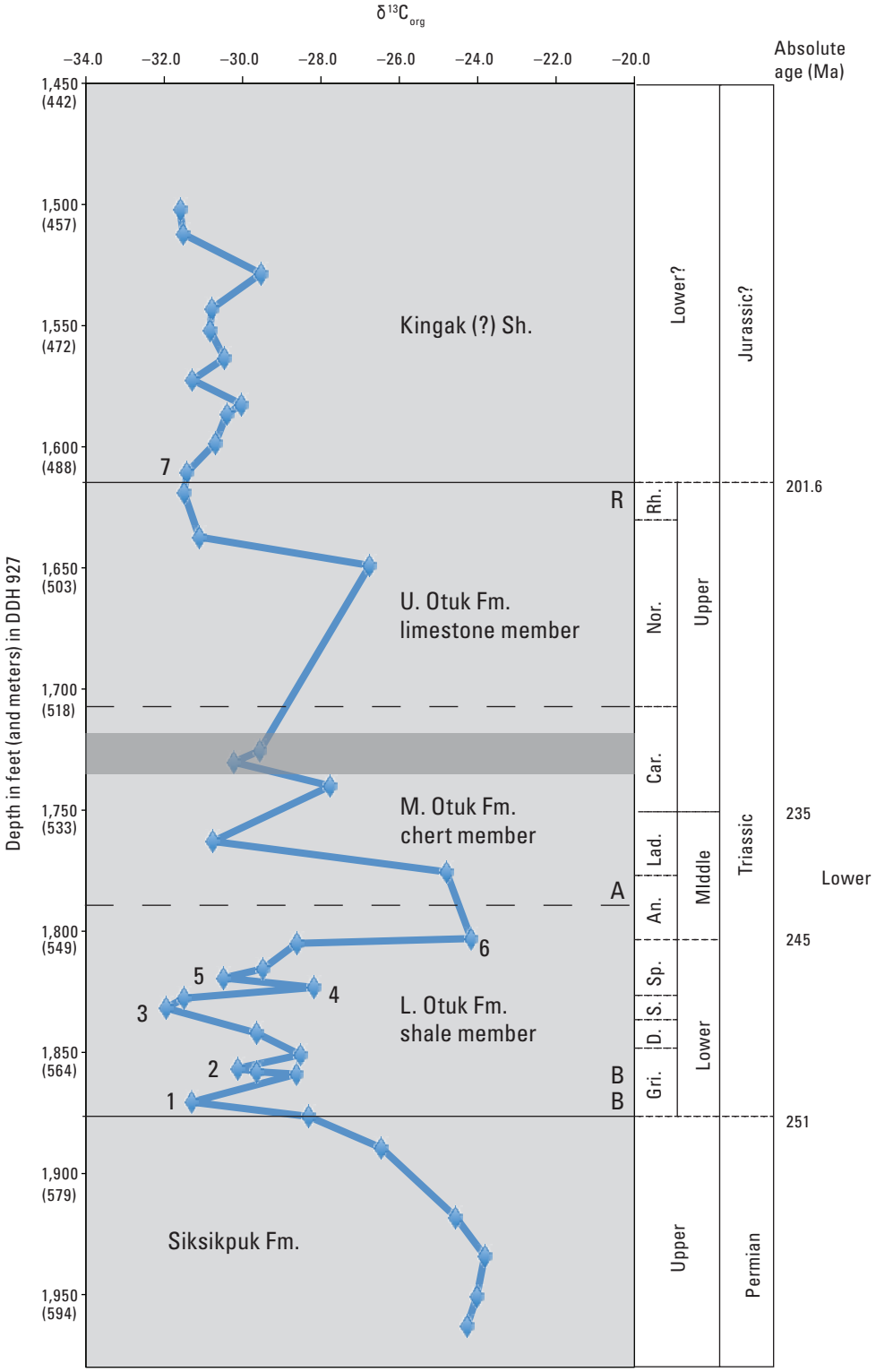

Figure 12. Diagram of $\delta^{13}C_{org}$ data from the upper Siksikpuk Formation through the Otuk Formation and into the Kingak(?) Shale in diamond-drill hole (DDH) 927. Dark band shows "marker horizon" of Young (2004)—dm in figure 6—which includes black shale with as much as 9.8 weight percent total organic carbon (TOC). B, bivalve fragments (?*Claraia* sp.) consistent with an earliest Griesbachian (earliest Triassic) age; A, Anisian radiolarians; R, late Rhaetian radiolarians. Numbers 1 through 7 indicate carbon isotope excursions (CIEs) discussed in the text. Placement of stage boundaries is constrained in the Lower Triassic by correlation of isotopic excursions, and in the Middle and Upper Triassic by radiolarian age data. Gri., Griesbachian; D., Dienerian; S., Smithian; Sp., Spathian; An., Anisian; Lad., Ladinian; Car., Carnian; Nor., Norian; Rh., Rhaetian. Griesbachian and Dienerian are equivalent to Induan Stage in Walker and Geissman (2009); Smithian and Spathian are equivalent to Olenekian Stage of these authors. U., upper; M., middle; L., lower. (See also tables 1, 2, and appendix.)

Table 2. Selected carbon isotope excursion (CIE) values from the Permian-Triassic boundary.

[DDH, diamond-drill hole; ‰, permil, or parts per thousand]

Data set	Excursion magnitude	Long-term offset	Estimated paleolatitude[1]	CIE data sources
DDH 927	−7.5‰	~ −5‰	~+45–60°	This paper
Fishburn-1, Australia	−8‰	−6.6‰	−40±6°	Morante (1996)
Paradise 1-6, Australia	−9.4‰	−7.7‰	−37±6°	Morante (1996)
Schuchert Dal, Greenland	−9‰	−6‰	+38±6°	Twitchett and others (2001)
Festningen, Spitsbergen	−5.6‰	−5.3‰	+46±6°	Wignall and others (1998)
Global average (range), marine rocks, *n*=14	−7±3.5‰ (−2.2 to −15‰)	(−0.3 to −7.7‰)		Retallack and Krull (2006)
Global average (range), marine and nonmarine rocks, *n*=30	−6.4±4.4‰ (−2.2 to −22.2‰)	(−0.3 to −7.7‰)		Retallack and Krull (2006)

[1]For DDH 927, from Scotese (2001), Lawver and others (2002), Kelly and others (2007), Colpron and Nelson (2009); all others from Retallack and Krull (2006).

(Young, 2004) and is well displayed in DDH 927. Basal Triassic (early Griesbachian) strata occur in the Ivishak Formation in the northeastern Brooks Range as denoted by the presence of *Claraia stachei* (Detterman and others, 1975; McRoberts, 2010). Bivalve fragments (*Claraia* sp.?) are found at several levels in the basal Otuk in DDH 927, including < 0.2 m below and <0.6 m above the peak of the negative carbon excursion (CIE 1; fig. 12); textural details of these fragments correlate well with those seen in photographs of *Claraia* cf. *stachei* in Boyd and Newell (1976).

Early Triassic

Another feature of the Otuk Formation $\delta^{13}C_{org}$ record that can be correlated globally is a series of negative and positive excursions in the shale member. Lower Triassic sections that have been studied in detail display a series of "abrupt and profound variations" in $\delta^{13}C_{org}$ and $\delta^{13}C_{carb}$ (Tanner, 2010, p. 108). Retallack and others (2005, p. 12) suggested that "the sequence and magnitude of carbon isotope negative excursions [in the Early Triassic] can be used like a bar code for international correlation." These authors document three negative $\delta^{13}C_{org}$ excursions above the system boundary event in nonmarine sections of Antarctica and list other localities where coeval excursions in $\delta^{13}C_{org}$ and $\delta^{13}C_{carb}$ can be found. The excursions and localities given by Retallack and others (2005) are (1) mid-Griesbachian (also in Austria, Armenia, Iran, Turkey, China, and Australia); (2) mid-Smithian (also in Utah, Pakistan, China, and Australia); and (3) end-Spathian (also in China). Tanner (2010) tabulated additional $\delta^{13}C_{carb}$ profiles that display these anomalies.

However, the $\delta^{13}C_{carb}$ data in Tanner (2010) also have two prominent positive anomalies that are thought to be global in extent; they span the Smithian-Spathian and Spathian-Anisian boundaries. These anomalies are absent from the $\delta^{13}C_{org}$ profiles in Retallack and others (2005) but are present in the $\delta^{13}C_{org}$ curve from Spitsbergen (Galfetti and others, 2007), although the Spathian-Anisian excursion in the Spitsbergen dataset is small.

Our isotope data from the shale member in DDH 927 define three distinct negative excursions above the boundary event (CIEs 2, 3, and 5, fig. 12) that occur within ~16 m (54 ft) of section and could be coeval with the excursions identified by Retallack and others (2005). This correlation suggests that CIEs 2, 3, and 5 (fig. 12) are of mid-Griesbachian, mid-Smithian, and late Spathian ages, respectively. These excursions have magnitudes of 1.5, 3.5, and 2.3‰ (fig. 12) which, like those in the Antarctic strata, are smaller than the boundary event excursion. Positive anomalies are also seen in the $\delta^{13}C_{org}$ data from DDH 927. There is a slight positive excursion between CIEs 3 and 5 that, if the age estimates above are correct, could represent the Smithian-Spathian boundary event (CIE 4, fig. 12). A much larger positive anomaly just above CIE 5 (CIE 6, fig. 12; >4‰) may be the Spathian-Anisian event; Anisian radiolarians were identified ~5 m above the start of this excursion (table 1, fig. 12).

Middle Through Early Late Triassic

Few $\delta^{13}C_{org}$ analyses have been published from strata of Middle through early Late Triassic (Anisian-Carnian) age. The $\delta^{13}C_{carb}$ curves available from this time indicate that, after the positive excursion at the base of the Anisian, uniformly low

values prevailed through most of the Middle Triassic (Tanner, 2010). Values began to rise near the top of the Ladinian, and continued to rise through the Carnian (data summarized in Tanner, 2010).

The Middle Triassic section in DDH 927 is chert rich and condensed. Sparse $\delta^{13}C_{org}$ values from this interval (fig. 12) are low near the base of the Ladinian, and then higher near the middle of the chert member, in strata that are likely Carnian. Lower values occur in the organic-rich marker horizon near the top of the member.

Triassic-Jurassic Boundary

A number of $\delta^{13}C_{org}$ profiles have been published for Norian and Rhaetian strata and the Triassic-Jurassic boundary. Data from western Canada suggest constant values across the Carnian-Norian boundary (Williford, Orchard, and others, 2007). Profiles across the Norian-Rhaetian boundary, also from western Canada, have been variously interpreted. Sephton and others (2002) reported a significant and extended positive excursion at this boundary in a section in British Columbia. Ward and others (2004) also reported a positive CIE from this time interval in the Queen Charlotte Islands, which they interpreted as coeval with the demise of monotid pectens and a shift from bioturbated to laminated facies. However, a more detailed reanalysis of the Queen Charlotte Islands section by Williford, Ward, and others (2007) indicated short-term variability but no clear excursion.

A significant negative excursion in $\delta^{13}C_{org}$ has been recognized at a number of marine sections near the Rhaetian-earliest Jurassic (Hettangian) boundary. Data summarized by Tanner (2010) from sections in England, Hungary, Nevada, and western Canada indicate an excursion of ~2 to 4‰ from a baseline of ~-26 to -29‰. In several of these sections, the negative CIE is followed by a strong positive excursion in the Hettangian (Tanner, 2010).

Carbon isotope data from Upper Triassic strata in DDH 927 are sparse, but a high $\delta^{13}C_{org}$ value (−26.8‰) was found in strata of latest Norian or earliest Rhaetian age that lack monotid bivalves (fig. 12). Much lower values occur near the top of the Otuk Formation and persist into the overlying Kingak(?) Shale (CIE 7, fig. 12). Values remain low throughout the Kingak(?) and mostly range from −30.4 to −31.6‰, with two slightly higher values of −29.5 and −30.0‰. Data from DDH 1110 (appendix, table A1) show a similar pattern. A single sample near the base of the limestone member, in rocks of middle or slightly older Norian age, has a relatively high value of −27.8‰. Much lower values (−30.1 to −30.9‰) occur in the uppermost Otuk, where three samples in strata of probable Rhaetian age define a negative trend. Even more depleted compositions (−31.2 to −33.5‰) are found through the overlying Kingak(?).

The low $\delta^{13}C_{org}$ values in the uppermost Otuk Formation in the Anarraaq drill holes may correlate with the negative excursion documented by Tanner (2010) at the Triassic-Jurassic boundary, but the sparsity of our data and the lack of age control for the Kingak(?) Shale render this interpretation uncertain. Our $\delta^{13}C_{org}$ profiles differ in several respects from those shown by Tanner (2010). Although our curves show negative shifts in the Late Triassic that are comparable in magnitude to shifts seen in other sections, radiolarian data indicate that shifts in the Red Dog area took place over a greater time span. Profiles in Tanner (2010) show sharp decreases of ~2 to 4‰ in the late Rhaetian. Curves in DDHs 927 and 1110 show decreases of similar magnitude (4.7‰ and 3.1‰, respectively), but these depletions began in the Norian and continued through the Rhaetian. In addition, only a moderate recovery (increase of ~1.5‰) is seen in the basal part of the Kingak(?) Shale in DDH 927. In DDH 1110, $\delta^{13}C_{org}$ values continue to decrease across the boundary into the Kingak(?), and then remain generally low (with some fluctuation) throughout the unit. Profiles in Tanner (2010) show values that increase by ~1.5 to 3‰ in the basal Hettangian, with even greater increases slightly higher in this stage. Regionally, the basal Kingak Shale is Hettangian (Houseknecht and Bird, 2004) and a Hettangian age for the basal Kingak(?) in the Anarraaq area is reasonable. But at present, there is no way to estimate how much of the Kingak(?) in these drill holes might be post-Hettangian, or to assess whether disconformities are present in the section. Additional isotope and biostratigraphic data from DDH 927 and 1110 may help to resolve these questions.

Isotopic Data from Correlative Sections

Preliminary $\delta^{13}C_{org}$ profiles from the Otuk Formation at Tiglukpuk Creek and from the Shublik Formation at Fire Creek were presented by Whalen and others (2006). The Fire Creek profile cannot readily be compared with the Red Dog profile, because the Shublik is mainly Middle Triassic and younger and relatively few isotopic data points of this age were obtained from the Otuk in DDH 927. However, the general stratigraphy of the Otuk at Tiglukpuk Creek is quite similar to that in the Anarraaq area, and the isotope profile is also similar. Neither the Sikiskpuk Formation nor the basal few meters of the Otuk were sampled at Tiglukpuk, but the profile begins with a negative offset that may correlate with the upper part of the Permian-Triassic boundary excursion. Three negative excursions occur above this in the shale member and could correlate with CIEs 2, 3, and 5 in the shale member in DDH 927, but a large positive excursion is seen above the lowest of these at Tiglukpuk that has no counterpart in the Anarraaq data set. Conversely, no equivalent of CIE 6 has been found at Tiglukpuk. As in the Anarraaq drill holes, $\delta^{13}C_{org}$ values at Tiglukpuk become depleted in the upper part of the Otuk, but the age of these strata is not well constrained; Rhaetian rocks may be absent (Bodnar, 1984; Kelly and others, 2007).

Conclusions

Our study of a complete, structurally uncomplicated subsurface section of the Otuk Formation in the Red Dog District in northwestern Alaska has implications for petroleum geology, regional paleogeography, and global carbon isotope stratigraphy. Here, in the structurally lowest (Wolverine Creek) plate of the EMA, the Otuk is ~82 m thick, gradationally overlies the Siksikpuk Formation, and conformably underlies the Kingak(?) Shale. The Otuk consists of shale, chert, and limestone members, and ranges from Early through latest Triassic (Rhaetian) age. Dark gray to black silty shale (1.3-6.9 weight percent TOC) makes up more than half of the shale member and ~10 to 15 percent of the lower chert member. A distinctive dark marker horizon, 2.4 m thick, near the top of the chert member is mostly dark mudstone with as much as 9.8 weight percent TOC. Dark shale (as much as 3.8 weight percent TOC) forms ~20 percent of the upper part of the limestone member. The Kingak(?) Shale is also organic-rich (1.3–6.5 weight percent TOC). These units accumulated mainly in outer shelf, poorly to moderately oxygenated settings; regional correlations suggest that lithofacies become increasingly distal in higher structural positions and within a single structural level from east to west. $\delta^{13}C_{org}$ data from the upper Siksikpuk through the Otuk and into the Kingak(?) Shale show negative and positive excursions strikingly similar to those reported for other Triassic sections. In particular, a large negative excursion at the base of the Otuk likely correlates with a marked excursion found at the Permian-Triassic boundary at many localities worldwide.

Acknowledgments

We thank the staff of the Teck and Cominco Mining Companies for permission to study their cores from the Red Dog District, and the Mineral Resources and Energy Resources Programs of the USGS for financial support of this study. We particularly acknowledge Karen Kelley, John Slack, and Craig Johnson (USGS) and Jeff Clark (Teck) for their help and discussions in the field and office. Thanks also to Keith Labay of the USGS for assistance with the figures and to Mike Whalen (University of Alaska, Fairbanks) for providing a version of figure 1, loaning thin sections of the Otuk Formation from Tiglukpuk Creek, and many useful discussions. Consultations with Tom Waller (U.S. National Museum) on Triassic bivalves are much appreciated. Use of company names does not constitute endorsement by the USGS.

References Cited

Berger, W.H., and Winterer, E.L., 1974, Plate stratigraphy and the fluctuating carbonate line: International Association of Sedimentologists Special Publication 1, p. 11–48.

Blodgett, R.B., and Bird, K., 2002, Megafossil biostratigraphy and T-R cycles of the Shublik Formation in the Phoenix #1 well, northern Alaska [abs.]: American Association of Petroleum Geologists Program and Abstracts, Pacific Section, p. 63.

Blome, C.D., 1983, Upper Triassic Capnuchosphaeridae and Capnodocinae from eastern Oregon: Micropaleontology, v. 29, no. 1, p. 11–49, 11 pls.

Blome, C.D., 1984, Upper Triassic Radiolaria and radiolarian zonation from western North America: Bulletins of American Paleontology, v. 85, no. 318, 88 p.

Blome, C.D., Reed, K.M, and Talilleur, I.L., 1988, Radiolarian biostratigraphy of the Otuk Formation in and near the National Petroleum Reserve in Alaska *in* Gryc, G., ed., Geology and exploration of the National Petroleum Reserve in Alaska, 1974–1982: U.S. Geological Survey Professional Paper 1399, p. 725–776.

Bodnar, D.A., 1984, Stratigraphy, age, depositional environments, and hydrocarbon source rock evaluation of the Otuk Formation, north-central Brooks Range, Alaska: Fairbanks, University of Alaska, unpublished master's thesis, 231 p.

Boyd, D.W., and Newell, N.D., 1976, Diagenetic image reversal in a Triassic pelecypod: Contributions to Geology, University of Wyoming, v. 14, no. 2, p. 65–68.

Campbell, R.H., 1967, Areal geology in the vicinity of the Chariot site, Lisburne Peninsula, northwestern Alaska: U.S. Geological Survey Professional Paper 395, 71 p., 2 sheets, scale 1:63,360.

Carter, E.S., 1993, Biochronology and paleontology of uppermost Triassic (Rhaetian) radiolarians, Queen Charlotte Islands, British Columbia, Canada: Mémoires de Géologie (Lusanne), no. 11, 175 p.

Colpron, M., and Nelson, J.L., 2009, A Palaeozoic northwest passage—Incursion of Caledonian, Baltican and Siberian terranes into eastern Panthalassa, and the early evolution of the North American Cordillera, *in* Cawood, P., and Kröner, A., eds., Earth accretionary systems in space and time: Geological Society of London Special Publication 318, p. 273-307.

Dennen, K.O., Johnson, C.A., Wandless, G.A., Otter, M.L., and Silva, S.R., 2006, $\delta^{15}N$ and non-carbonate $\delta^{13}C$ values for two petroleum source rock reference materials and a marine sediment reference material: U.S. Geological Survey Open-File Report 2006-1071, 14 p.

Detterman, R.L., Reiser, H.N., Brosgé, W.P., and Dutro, J.T., Jr., 1975, Post-Carboniferous stratigraphy, northeastern Alaska: U.S. Geological Survey Professional Paper 886, 46 p.

De Vera, Jose, McClay, K.R., and King, A.R., 2004, Structure of the Red Dog district, western Brooks Range, Alaska: Economic Geology, v. 99, p. 1415-1434.

Dumoulin, J.A., Harris, A.G., Blome, C.D., and Young, L.E., 2004, Depositional settings, correlation, and age of Carboniferous rocks in the western Brooks Range, Alaska: Economic Geology, v. 99, p. 1355-1384.

Dumoulin, J.A., Harris, A.G., Blome, C.D., and Young, L.E., 2006, Conodont and radiolarian data from the De Long Mountains quadrangle and adjacent areas: U.S. Geological Survey Open-File Report 2006-1068, accessed November 8, 2011, at http://pubs.usgs.gov/of/2006/1068/.

Dumoulin, J.A., and White T., 2005, Micromorphological evidence for paleosol development in the Endicott Group, Siksikpuk Formation, Kingak(?) Shale, and Ipewik Formation, western Brooks Range, Alaska, *in* Haeussler, P., and Galloway, J., eds., Studies by the U.S. Geological Survey in Alaska, 2004: U.S. Geological Survey Professional Paper 1709–E, accessed November 8, 2011, at http://pubs.usgs.gov/pp/pp1709e/.

Galfetti, T., Hochuli, P.A., Brayard, A., Bucher, H., Weissart, H., and Vigran, J.O., 2007, Smithian/Spathian boundary event: evidence for global climatic change in the wake of the end-Permian biotic crisis: Geology, v. 35, p. 291–294.

Hallam, A., 1996, Major bio-events in the Triassic and Jurassic, *in* Walliser, O.H., ed., Global events and event stratigraphy in the Phanerozoic: Springer Verlag, p. 265–283.

Houseknecht, D.W., 2001, Sequence stratigraphy and sedimentology of Beaufortian strata (Jurassic-Lower Cretaceous) in the National Petroleum Reserve - Alaska, *in* Houseknecht, D.W., ed., NPRA Core Workshop; Petroleum Plays and Systems in the National Petroleum Reserve - Alaska, SEPM Core Workshop No. 21, p. 57–88.

Houseknecht, D.W., and Bird, K.J., 2004, Sequence stratigraphy of the Kingak Shale (Jurassic-Lower Cretaceous), National Petroleum Reserve in Alaska: American Association of Petroleum Geologists Bulletin, v. 88, no. 3, p. 279–302.

Hubbard, R.J., Edrich, S.P., and Rattey, R.P., 1987, Geologic evolution and hydrocarbon habitat of the "Arctic Alaska microplate": Marine and Petroleum Geology, v. 4, no. 1, p. 2–34.

Johnson, C.A., Kelley, K.D., and Leach, D.L., 2004, Sulfur and oxygen isotopes in barite deposits of the western Brooks Range, Alaska, and implications for the origin of the Red Dog massive sulfide deposits: Economic Geology, v. 99, p. 1435–1448.

Kelly, L.N., 2004, High resolution sequence stratigraphy and geochemistry of Middle and Upper Triassic sedimentary rocks, northeastern and northcentral Brooks Range, Alaska: Fairbanks, University of Alaska, unpublished master's thesis,199 p.

Kelly, L.N., Whalen, M.T., McRoberts, C.A., Hopkin, E., and Tomsich, C.S., 2007, Sequence stratigraphy and geochemistry of the upper Lower through Upper Triassic of northern Alaska—Implications for paleoredox history, source rock accumulation, and paleoceanography: Alaska Division of Geological and Geophysical Surveys Report of Investigations 2007-1, 50 p.

Krull, E.S., Lehrmann, D.J., Druke, D., Kessel, B., YouYi, Y., and Rongxi, L., 2004, Stable carbon isotope stratigraphy across the Permian-Triassic boundary in shallow marine carbonate platforms, Nanpanjiang Basin, south China: Palaeogeography, Palaeoclimatology, Palaeoecology, v. 204, p. 279–315.

Lawver, L.A., Grantz, A., and Gahagan, L.M., 2002, Plate kinematic evolution of the present Arctic region since the Ordovician, *in* Miller, E.L., Grantz, A., and Klemperer, S.L., eds., Tectonic evolution of the Bering Shelf-Chukchi Sea-Arctic margin and adjacent landmasses: Geological Society of America Special Paper 360, p. 333–358.

Lillis, P.G., 2003, Representative bulk composition of oil types for the 2002 U.S. Geological Survey Resource Assessment of National Petroleum Reserve in Alaska: U.S. Geological Survey Open-File Report 03-407, accessed November 8, 2011, at http://pubs.usgs.gov/of/2003/of03-407/.

Lillis, P.G., King, J.D., Warden, A., and Pribil, M.J., 2002, Oil-source rock correlation studies, central Brooks Range foothills and National Petroleum Reserve, Alaska (NPRA) [abs.]: American Association of Petroleum Geologists Program and Abstracts, Pacific Section, p. 89.

Magoon, L.B., and Bird, K.J., 1988, Evaluation of petroleum source rocks in the National Petroleum Reserve in Alaska, using organic-carbon content, hydrocarbon content, visual kerogen, and vitrinite reflectance, *in* Gryc, G., ed., Geology and exploration of the National Petroleum Reserve in Alaska, 1974 to 1982, U.S. Geological Survey Professional Paper 1399, p. 381–450.

Magoon, L.B., Woodward, P.V., Banet, A.C., Jr., Griscom, S.B., and Daws, T.A., 1987, Thermal maturity, richness, and type of organic matter of source-rock units, *in* Bird, K.J., and Magoon, L.B., eds., Petroleum geology of the northern part of the Arctic National Wildlife Refuge, northeastern Alaska: U.S. Geological Survey Bulletin 1778, p. 127–180.

Mayfield, C.F., Curtis, S.M., Ellersieck, I., and Tailleur, I.L., 1990, Reconnaissance geologic map of the De Long Mountains A-3 and B-3 quadrangles and parts of the A-4 and B-4 quadrangles, Alaska: U.S. Geological Survey Miscellaneous Investigations Series Map I-1929, 2 sheets, scale 1:63,360.

Mayfield, C.F., Tailleur, I.L., and Ellersieck, I., 1988, Stratigraphy, structure, and palinspastic synthesis of the western Brooks Range, northwestern Alaska, *in* Gryc, G., ed., Geology and exploration of the National Petroleum Reserve in Alaska, 1974-1982: U.S. Geological Survey Professional Paper 1399, p. 143–186.

McRoberts, C.A., 2010, Biochronology of Triassic bivalves, *in* Lucas, S.G., ed., The Triassic Timescale, Geological Society of London Special Publications, v. 334, p. 201–219.

Miller, E.L., Toro, J., Gehrels, G., Amato, J.M., Prokopiev, A., Tuchkova, M.I., Akinin, V.V., Dumitru, T.A., Moore, T.E., and Cecile, M.P., 2006, New insights into Arctic paleogeography and tectonics from U-Pb detrital zircon geochronology: Tectonics, v. 25, TC3013, doi:10.1029/2005TC001830.

Moore, T.E., Dumitru, T.A., Adams, K.E., Witebsky, S.N., and Harris, A.G., 2002, Origin of the Lisburne Hills-Herald Arch structural belt: Stratigraphic, structural, and fission-track evidence from the Cape Lisburne area, northwestern Alaska: Geological Society of America Special Paper 360, p. 77–109.

Morante, R., 1996, Permian and Early Triassic isotopic records of carbon and strontium in Australia and a scenario of events about the Permian-Triassic boundary: Historical Biology, v. 11, p. 289–310.

Mull, C.G., Tailleur, I.L., Mayfield, C.F., Ellersieck, I., and Curtis, S., 1982, New upper Paleozoic and Mesozoic stratigraphic units, central and western Brooks Range, Alaska: American Association of Petroleum Geologists Bulletin, v. 66, p. 348–362.

Ohtaka, M., Aita, Y., and Sakai, T., 1998, Middle Triassic radiolarian biostratigraphy of the bedded chert in the Minowa quarry, Kuzuu Town, Ashio Mountains: News of Osaka Micropaleontologists, Special Voume 11, p. 95–113.

Orchard, M.J., 2010, Triassic conodonts and their role in stage boundary definition, *in* Lucas, S.G., ed., The Triassic timescale: Geological Society of London Special Publications, v. 334, p. 139–161.

Parrish, J.T., Droser, M.L., and Bottjer, D.J., 2001, A Triassic upwelling zone—The Shublik Formation, Arctic Alaska, U.S.A.: Journal of Sedimentary Research, v. 71, p. 272–285.

Pessagno, E.A., Jr., 1979, Systematic Paleontology, *in* Pessagno, E.A., Jr., Finch, J.W., and Abbott, P.L., Upper Triassic Radiolaria from the San Hipolito Formation, Baja California: Micropaleontology, v. 25, no. 2, p. 160-197, pls. 1–9.

Pessagno, E.A., Jr., Finch, W., and Abbott, P.L., 1979, Upper Triassic Radiolaria from the San Hipólito Formation, Baja California: Micropaleontology, v. 25, p. 160–197.

Retallack, G.J., Jahren, A.H., Sheldon, N.D., Chakrabarti, R., Metzger, C.A., and Smith, R.M.H., 2005, The Permian-Triassic boundary in Antarctica: Antarctic Science, v. 17, no. 2, p. 1–18.

Retallack, G.J., and Krull, E.S., 2006, Carbon isotopic evidence for terminal-Permian methane outbursts and their role in extinction of animals, plants, coral reefs and peat swamps, *in* Greb, S.F., and DiMichele, W.A., eds., Wetlands through time: Geological Society of America Special Paper 399, p. 249–268.

Robison, V.D., Liro, L.M., Robison, C.R., Dawson, W.C., and Russo, J.W., 1996, Integrated geochemistry, organic petrology, and sequence stratigraphy of the Triassic Shublik Formation, Tenneco Phoenix #1 well, North Slope, Alaska, U.S.A.: Organic Geochemistry, v. 24, p. 257–272.

Sashida, K., Nishimura, H., Igo, H., Kazama, S., and Kamata, T., 1993, Triassic radiolarian faunas from Kisofukushima, Kiso Mountains, central Japan: Science Reports of the Institute of Geoscience, University of Tsukuba, section B, v. 14, p. 77–97.

Scotese, C.R., 2001, Atlas of Earth History, v. 1, Paleogeography PALEOMAP Project: Arlington, Texas, 52 p. (Also available at http://www.scotese.com/.)

Sephton, M.A., Amor, K., Franchi, I.A., Wignall, P.B., Newton, R., and Zonneveld, J.-P., 2002, Carbon and nitrogen isotope disturbances and an end-Norian (Late Triassic) extinction event: Geology, v. 30, p. 1119–1122.

Sugiyama, K., 1997, Triassic and Lower Jurassic radiolarian biostratigraphy in the siliceous claystone and bedded chert units of the southeastern Mino terrane: Bulletin of the Mizunami Fossil Museum, no. 24, p. 79–193.

Tanner, L.H., 2010, The Triassic isotope record, *in* Lucas, S.G., ed., The Triassic timescale, Geological Society of London Special Publications, v. 334, p. 103–118.

Tappan, H., 1951, Foraminifera from the Arctic slope of Alaska: U.S. Geological Survey Professional Paper 236–A, 20 p.

Twitchett, R.J., Looy, C.V., Morante, R., Visscher, H., and Wignall, P.B., 2001, Rapid and synchronous collapse of marine and terrestrial ecosystems during the end-Permian biotic crisis: Geology, v. 29, p. 351–354.

Walker, J.D., and Geissman, J.W., comps., 2009, GSA Geologic time scale: Geological Society of America, accessed November 8, 2011, at http://www.geosociety.org/science/timescale/.

Ward, P.D., Garrison, G.H., Haggart, J.W., Kring, D.A., and Beattie, M.J., 2004, Isotopic evidence bearing on Late Triassic extinction events, Queen Charlotte Islands, Brtish Columbia, and implications for the duration and cause of the Triassic-Jurassic mass extinction: Earth and Planetary Science Letters, v. 224, p. 589–600.

Whalen, M.T., Kelly, L., Hulm, E., Burruss, R.C., and Dumoulin, J.A., 2006, Sequence stratigraphy and geochemistry of the marine Triassic of Arctic Alaska, implications for Mesozoic paleogeography and paleoceanography [abs.]: Geological Society of America Abstracts with Program, v. 38, no. 5, p. 86.

Whidden, K.J., Dumoulin, J.A., Whalen, M.T., Hutton, E., and Moore, T.E., 2012, Distal facies variability within the Upper Triassic Part of the Otuk Formation in northern Alaska [abs.]: American Association of Petroleum Geologists (AAPG) Annual Convention and Exhibition, AAPG Search and Discovery Article 90142.

Wignall, P.B., Morante, R., and Newton, R., 1998, The Permo-Triassic transition in Spitsbergen: $\delta^{13}C_{org}$ chemostratigraphy, Fe and S geochemistry, facies, fauna, and trace fossils: Geological Magazine, v. 135, p. 47–62.

Williford, K.H. Orchard, M.J., Zonneveld, J.-P., McRoberts, C.A., and Beatty, T.W., 2007, A record of stable organic carbon isotopes from the Carnian-Norian boundary section at Black Bear Ridge, Williston Lake, British Columbia, Canada: Albertiana, v. 36, p. 146–148.

Williford, K.H., Ward, P.D., Garrison, G.H., and Buick, R., 2007, An extended organic carbon-isotope record across the Triassic-Jurassic boundary in the Queen Charlotte Islands, British Columbia, Canada: Palaeogeography, Palaeoclimatology, Palaeoecology, v. 244, p. 290–296.

Yeh, K.-Y., 1992, Triassic Radiolaria from Uson Island, Philippines: Bulletin of the National Museum of Natural Science, Taiwan, no. 3, p. 51–91.

Young, L.E., 2004, A geologic framework for mineralization in the western Brooks Range, Alaska: Economic Geology, v. 99, p. 1281–1306.

Appendix—Samples and Methods for Organic Carbon Analysis

Samples of drill core (1–2 cm thick) were collected at specific measured depths in the core. All samples from DDHs 927 and 1110 and analytical results of measurements of TOC and $\delta^{13}C_{org}$ are given in table A1. Unless indicated as single measurements, all results in table A1 are means and standard deviations for 2 to 5 analyses of each sample.

Core samples were sent to Geochemical Testing, Inc., for grinding and initial measurement of weight percent TOC. Ground samples were dried at 60 °C (degrees Celsius); multiple aliquots of each sample were weighed into silver foil cups and fumigated with HCl vapor to remove carbonate carbon as described in Dennen and others (2006). Fumigated samples were dried and silver cups containing powdered samples were distributed to USGS laboratories in Reston, Virginia, Denver, Colorado, and Menlo Park, California as well as to the Woods Hole Oceanographic Institution in Massachusetts. Analytical standards, described in Dennen and others (2006), were prepared in the same way and distributed to each laboratory for analysis with the unknowns.

Isotopic measurements were made by combustion of the samples in an elemental analyzer coupled to a continuous-flow isotope ratio mass spectrometer. The results are reported in δ-notation, where δ (in per mil) = $((R_{SA}-R_{ST})/R_{ST}) \times 1{,}000$, and R_{SA} and R_{ST} refer to the ratio $^{13}C/^{12}C$ in the sample and the Vienna Pee Dee Belemnite standard (VPDB), respectively.

Standard deviations averaged ±0.45‰, which is larger than the standard deviation of ±0.1‰ reported by Dennen and others (2006) for standards. This is assumed to reflect heterogeneity in the samples. Note that the largest standard deviations (table A1) correspond to samples with the lowest content of TOC, which are the most difficult to analyze precisely.

Table A1. Organic carbon data from diamond-drill holes (DDHs) 927 and 1110.

[cm, chert member; lm, limestone member; sm, shale member; TOC, total organic carbon; C, carbon; wt%, weight percent; Std. dev., standard deviation]

Field ID	Diamond-drill hole (DDH)	Unit	Core depth, in feet	TOC		Carbon isotopes	
				Mean wt% C	Std. dev. wt% C	Mean $\delta^{13}C$	Std. dev. $\delta^{13}C$
04RCB23	927	Kingak(?)	1,502	2.04	0.14	−31.6	0.28
04RCB22	927	Kingak(?)	1,512.1	3.7	0.013	−31.5	0.163
04RCB21	927	Kingak(?)	1,528.5	1.3	0.001	−29.5	0.527
04RCB20	927	Kingak(?)	1,543	1.7	0.001	−30.8	0.177
02RCB46	927	Kingak(?)	1,552.0	2.02	0.16	−30.8	0.35
02RCB45	927	Kingak(?)	1,563.5	1.76	0.24	−30.5	0.40
02RCB44	927	Kingak(?)	1,572.4	2.11	0.28	−31.3	0.50
02RCB43	927	Kingak(?)	1,582.5	1.32	0.07	−30.0	0.33
02RCB42	927	Kingak(?)	1,586.5	1.47	0.12	−30.4	0.33
02RCB41	927	Kingak(?)	1,598.5	1.66	0.36	−30.7	0.36
02RCB30	927	Kingak(?)	1,610.5	3.67	0.55	−31.4	0.46
04RCB18	927	Otuk lm	1,619	1.2	0.041	−31.5	0.099
04RCB19	927	Otuk lm	1,637.3	3.4	0.085	−31.1	0.441
02RCB28	927	Otuk lm	1,649	0.24	0.01	−26.8	1.68
04RCB15	927	Otuk cm	1,725.5	9.8	0.852	−29.6	0.146
02RCB26	927	Otuk cm	1,730.2	2.48	0.23	−30.2	0.36
04RCB14	927	Otuk cm	1,740	0.3	single value	−27.8	single value
04RCB13	927	Otuk cm	1,762.9	5.78	0.18	−30.8	0.33
04RCB01	927	Otuk cm	1,775.5	0.2	0.011	−24.8	0.087

Table A1. Organic carbon data from diamond-drill holes (DDHs) 927 and 1110.—Continued

[cm, chert member; lm, limestone member; sm, shale member; TOC, total organic carbon; C, carbon; wt%, weight percent; Std. dev., standard deviation]

Field ID	Diamond-drill hole (DDH)	Unit	Core depth, in feet	TOC		Carbon isotopes	
				Mean wt% C	Std. dev. wt% C	Mean $\delta^{13}C$	Std. dev. $\delta^{13}C$
04RCB02	927	Otuk sm	1,803	0.25	0.02	−24.2	0.87
02RCB24	927	Otuk sm	1,805	0.12	0.06	−28.6	1.95
02RCB23	927	Otuk sm	1,815.5	5.77	0.59	−29.5	0.39
04RCB03	927	Otuk sm	1,819.3	6.51	0.66	−30.5	0.28
02RCB22	927	Otuk sm	1,823.2	6.85	0.42	−28.2	0.49
04RCB04	927	Otuk sm	1,827.6	1.29	0.08	−31.5	0.32
02RCB21	927	Otuk sm	1,831.7	2.94	0.09	−32.0	0.41
02RCB20	927	Otuk sm	1,842	0.19	0.13	−29.6	1.27
02RCB18	927	Otuk sm	1,851	0.19	0.05	−28.5	1.00
02RCB13	927	Otuk sm	1,856.6	3.22	0.24	−30.1	0.14
02RCB17	927	Otuk sm	1,858	2.43	0.17	−29.6	0.06
02RCB19	927	Otuk sm	1,859	2.40	0.19	−28.6	0.22
04RCB05	927	Otuk sm	1,870.5	3.2	0.065	−31.3	0.254
04RCB06	927	Otuk sm	1,876.5	1.4	0.001	−28.3	0.237
04RCB07	927	Siksikpuk	1,889.5	0.3	0.002	−26.5	0.043
04RCB09	927	Siksikpuk	1,918	0.2	0.001	−24.6	0.346
04RCB10	927	Siksikpuk	1,934	0.6	0.003	−23.8	0.041
04RCB11	927	Siksikpuk	1,950.7	0.2	0.008	−24.0	0.126
04RCB12	927	Siksikpuk	1,963	0.4	single value	−24.3	single value
04RCB66	1110	Okpikruak	1,931.5	1.82	0.09	−31.26	0.34
04RCB65	1110	Okpikruak	1,935.0	0.37	0.01	−30.49	0.95
04RCB64	1110	Kingak(?)	1,939.5	2.52	0.02	−33.46	1.69
04RCB63	1110	Kingak(?)	1,943.8	4.69	0.12	−32.53	0.39
04RCB62	1110	Kingak(?)	1,959.0	6.53	0.11	−32.80	0.30
04RCB61	1110	Kingak(?)	1,967.0	3.84	0.06	−33.12	0.53
02RCB50	1110	Kingak(?)	1,972.0	3.14	single value	−31.34	single value
04RCB60	1110	Kingak(?)	1,987.0	3.51	0.06	−32.59	0.29
04RCB59	1110	Kingak(?)	2,009.0	4.01	0.04	−32.15	0.65
02RCB51	1110	Kingak(?)	2,019	2.10	0.13	−31.24	0.09
04RCB58	1110	Kingak(?)	2,026	2.4	0.1	−31.2	0.3
04RCB57	1110	Kingak(?)	2,038.0	2.50	0.11	−31.65	0.39
04RCB56	1110	Kingak(?)	2,045.0	2.24	0.10	−31.51	0.36
04RCB55	1110	Otuk lm	2,046.5	1.92	0.06	−30.92	0.40
04RCB54	1110	Otuk lm	2,052	3.7	0.2	−30.4	0.3
04RCB53	1110	Otuk lm	2,059.3	2.01	0.11	−30.09	0.43
04RCB52	1110	Otuk lm	2,072.5	3.78	0.03	−30.91	0.27
04RCB46	1110	Otuk lm	2,184	0.2	0.0	−27.8	0.8

Menlo Park Publishing Service Center, California
Manuscript approved for publication April 23, 2013
Edited by James W. Hendley II
Layout and design by James E. Banton